Performance assessment of three convective parameterization schemes in WRF for downscaling summer rainfall over South Africa

Satyaban B. Ratna, J. V. Ratnam, S. K. Behera, C. J. deW. Rautenbach, T. Ndarana, K. Takahashi and **T. Yamagata**

Abstract Austral summer rainfall over the period 1991/1992 to 2010/2011 was dynamically downscaled by the weather research and forecasting (WRF) model at 9 km resolution for South Africa. Lateral boundary conditions for WRF were provided from the European Centre for medium-range weather (ECMWF) reanalysis (ERA) interim data. The model biases for the rainfall were eval-uated over the South Africa as a whole and its nine prov-inces separately by employing three different convective parameterization schemes, namely the (1) Kain–Fritsch (KF), (2) Betts–Miller–Janjic (BMJ) and (3) Grell–Devenyi ensemble (GDE) schemes. All three schemes have gener-ated positive rainfall biases over South Africa, with the KF scheme producing the largest biases and mean absolute errors. Only the BMJ scheme could reproduce the intensity of rainfall anomalies, and also exhibited the highest cor-relation with observed interannual summer rainfall vari-ability. In the KF scheme, a significantly high amount of moisture was transported from the tropics into South Africa. The vertical thermodynamic profiles show that the KF scheme has caused low level moisture convergence, due to the highly unstable atmosphere, and hence con-tributed to the widespread positive biases of rainfall. The negative bias in moisture, along with a stable atmosphere and negative biases of vertical velocity simulated by the GDE scheme resulted in negative rainfall biases, especially over the Limpopo Province. In terms of rain rate, the KF scheme generated the lowest number of low rain rates and the maximum number of moderate to high rain rates associated with more convective unstable environment. KF and GDE schemes overestimated the convective rain and underestimated the stratiform rain. However, the simulated convective and stratiform rain with BMJ scheme is in more agreement with the observations. This study also docu-ments the performance of regional model in downscaling the large scale climate mode such as El Nin˜o Southern Oscillation (ENSO) and subtropical dipole modes. The correlations between the simulated area averaged rainfalls over South Africa and Nino3.4 index were -0.66, -0.69 and -0.49 with KF, BMJ and GDE scheme respectively as compared to the observed correlation of -0.57. The model could reproduce the observed ENSO-South Africa rainfall relationship and could successfully simulate three wet (dry) years that are associated with La Nin˜a (El Ni˜no) and the BMJ scheme is closest to the observed variability. Also, the model showed good skill in simulating the excess rainfall over South Africa that is associated with positive sub-tropical Indian Ocean Dipole for the DJF season 2005/2006.

Keywords South Africa ; WRF regional model ; ENSO ; Seasonal rainfall ; Convective parameterization schemes ; Downscaling

S. B. Ratna (Correspondence author) · J. V. Ratnam · S. K. Behera · K. Takahashi · T. Yamagata
Application Laboratory, Yokohama Institute for Earth Sciences, JAMSTEC, 3173-25 Showa-machi, Kanazawa-ku, Yokohama, Kanagawa 236-0001, Japan
e-mail: satyaban14@gmail.com

J. V. Ratnam · S. K. Behera
Research Institute for Global Change, JAMSTEC, Yokohama, Japan

C. J. deW.Rautenbach
University of Pretoria, Pretoria, South Africa

T. Ndarana
South African Weather Service, Pretoria, South Africa

K. Takahashi
Earth Simulator Center, JAMSTEC, Yokohama, Japan

1 Introduction

South Africa is characterized by complex topographical features and marked gradients in vegetation and land cover, and receives most of its rainfall during the austral summer season (December–January–February: DJF), when tropical temperate troughs (TTTs), westerly troughs, cut off low pressure systems and thunderstorms (van Heerden and Taljaard 1998) dominate. The country is located in the dry subtropics of the Southern Hemisphere, meaning that rainfall exhibits large spatio-temporal variability modulated by both tropical and mid-latitudinal dynamics. Because of its influence on social society, the economy (in particular agriculture) and water resource planning, the understanding and prediction of summer rainfall variability is regarded as a high priority.

As part of global rainfall-sea surface temperature (SST) teleconnection (e.g. arising from the El Nin˜o Southern Oscillation (ENSO), the Indian Ocean Dipole (IOD), the subtropical dipoles in Indian and Atlantic Oceans), South African rainfall is influenced through ocean–atmosphere boundary forcing on synoptic-scale atmospheric dynamics (Mutemi et al. 2007; Ratna et al. 2013). The complexity of these teleconnection often makes it difficult to produce reliable seasonal rainfall predictions.

Despite of the development of many global general circulation model (GCM) systems for long-term seasonal rainfall predictions, the skill still remains a challenge. The improvement of rainfall simulations by GCMs therefore remains an imperative topic of research. An important aspect of improving rainfall output from GCM simulations is to resolve the regional heterogeneity of rain contributing variables on higher resolutions (Giorgi and Mearns 1999), but this often requires abundant computer resources. A more applicable approach is to dynamically downscale rainfall from GCMs by the nesting of higher resolution regional climate models (RCMs) into GCM simulations (Leung et al. 2003). Since the mid-1990s many RCM sensitivity studies on domain location and size, initial and lateral boundary conditions, horizontal and vertical grid resolutions and model physics have been conducted. It was found that the use of RCMs could result in improved atmospheric simulations since their dynamics and physics were capable to desegregate climate data at higher resolutions, although simulation uncertainties related to, for example, physical parameterization schemes, still remain.

Before applying a RCM for seasonal prediction for a given region, the accuracy of the model in reproducing the observed regional climate should be assessed in order to establish the model's strengths and weaknesses. This could be achieved by using historically observed data as lateral boundary forcing to the RCM (Giorgi and Mearns 1999). It is known that convective rainfall is more dominant over South Africa during summer months, implying that the evaluation of convective parameterization schemes applied to specific spatial resolutions in a RCM is pertinent. As a matter of fact, many studies emphasized the strong sensitivity of simulated regional climate to physical parameterization schemes used in RCMs (e.g. Cre´tat et al. 2011). Despite of this, the evaluation of RCM convective parameterization schemes for simulations over southern Africa is still very limited.

RCMs have previously been used as dynamical downscaling aids for studying regional climates over southern Africa (Joubert et al. 1999; Engelbrecht et al. 2002; Hud-son and Jones 2002; Tadross et al. 2006; Kgatuke et al. 2008; Landman et al. 2009). The weather research and forecasting (WRF) model (Skamarock et al. 2008) i s increasingly being used as RCM for downscaling studies over southern Africa (Cre´tat et al. 2011, 2012; Ratnam et al. 2012, 2013; Cre´tat and Pohl 2012; Boulard et al. 2012; Vigaud et al. 2012). However, previous WRF sim-ulations aimed at studying summer rainfall over southern Africa consist of either relatively coarse grid resolutions, or addressed only a few seasons. Furthermore, none of the studies addressed rainfall distribution on a subregional scale over the different provinces of South Africa and its sensitivity to different convective schemes. It was found that horizontal resolutions of between 25 and 50 km are insufficient to represent fundamental and persistent atmo-spheric process associated with the convective boundary layer or irregular coastlines and topography (Kanamaru and Kanamitsu 2007; Kanamitsu and Kanamaru 2007; Caldwell et al. 2009; Barstad et al. 2009; Heikkila et al. 2011). Soares et al. (2012) also found that a higher grid resolution allowed for improved simulations of extreme rainfall events.

The main aim of this study is to evaluate the WRF model in simulating the summer rainfall over South Africa and also to evaluate the fidelity of the model in simulating the interannual variability in the summer rainfall. To achieve the goal, WRF model was run for twenty austral summer seasons (DJF; 1991/1992–2010/2011) using two way nested domains at a horizontal resolution of 27 and 9 km. As the model simulations are sensitive to the cumulus parameterization schemes used in the model, we made the model run with three convective schemes for all the 20 years. The 9 km domain simulated model precipitation biases and the causes of the biases are presented in the following sections.

2 Model, experimental design and data

Weather research and forecasting (WRF) model (Advanced Research WRF (ARW); version 3.4) developed by the

national centre for atmospheric research (NCAR) (Skamarock et al. 2008), is used in this study. WRF model is a non-hydrostatic, fully compressible and terrain-following sigma coordinate model. In this study WRF simulations over South Africa are performed using a two way nested domain with horizontal resolutions of 27 and 9 km (Fig. 1). Both the domains have 28 sigma levels in the vertical with upper boundary at 10 hPa. The WRF domain with 27 km horizontal resolution covers southern Africa as well as parts of the surrounding Atlantic and Indian Oceans (0.6°E–60.3°E, 8.4°S–44.6°S) with 215 grid points in the east–west and 150 grid points in north–south directions. The nested inner domain with a 9 km horizontal resolution covers South Africa its neighboring countries (10.9°E–38.0°E, 19.4°S–36.5°S) with 292 grid points in the east–west and 211 grid points in north–south directions.

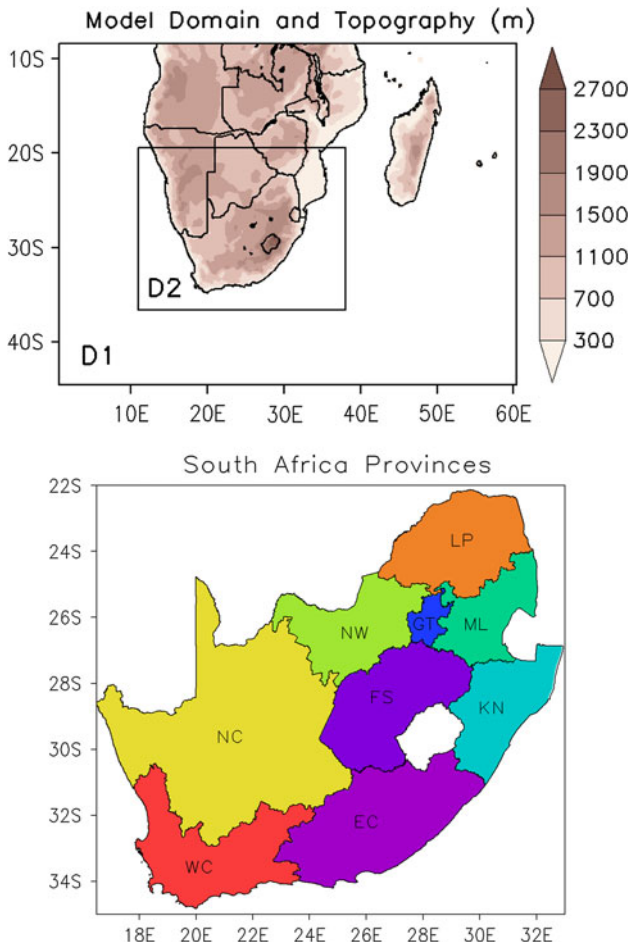

Fig. 1 Weather research and forecasting (WRF) model domains considered in this study with a 27 km (D1) and 9 km (D2) horizontal grid resolution (*top*). Topography (expressed in meters above mean sea level) is *shaded*. At the *bottom* are the nine Provinces of South Africa (*LP* Limpopo, *NW* North West, *NC* Northern Cape, *FS* Free State, *GT* Gauteng, *ML* Mpumalanga, *KN* KwaZulu-Natal, *EC* Eastern Cape and *WC* Western Cape Provinces)

Physical parameterization schemes considered include the microphysics scheme of the WSM 3-class simple ice scheme (Hong et al. 2004), the Unified NOAH scheme for land surface processes (Chen and Dudhia 2001), the Yonsei University scheme for the planetary boundary layer (PBL) (Noh et al. 2003), the rapid radiative transfer model (RRTM) scheme for long waves (Mlawer et al. 1997) and the Dudhia scheme for short waves (Dudhia 1989). The choice of these physics packages is consistent with what Cre´tat et al. (2011) and Ratnam et al. (2012) previously used for simulation of the climate of southern Africa.

This study aims at investigating the skill of different convective parameterization schemes in reproducing summer rainfall over South Africa and its provinces. For this purpose, three convective parameterization schemes were considered, namely: (1) the Kain–Fritsch (KF) (Kain 2004); (2) the Betts–Miller–Janjic (BMJ) (Betts and Miller 1986; Janjic 1994); and (3) the Grell–Devenyi ensemble (GDE) (Grell and De´ve´nyi 2002) scheme. The KF scheme describes both deep and shallow sub-grid convection using a mass flux approach with downdrafts and a convective available potential energy (CAPE) removal timescale. Its trigger is based on the grid resolved vertical motion (Kain and Fritsch 1993). The BM scheme is exclusively driven by the thermodynamics at a given model grid point, in which conditional instability is removed by adjusting the temperatures and specific humidities toward a reference profile (approximately a moist adiabat) within a specified timescale (Betts and Miller 1986). The GDE scheme employs a multi-closure, multi-parameter, ensemble method with typically 144 sub-grid members (Grell and De´ve´nyi 2002).

The 6 hourly, 0.75° × 0.75° grid European Centre for medium-range weather (ECMWF) reanalysis (ERA) interim data (Dee et al. 2011) was used as the initial and boundary conditions for the simulations. The main advantage of the ERA interim data, compared to the pre-vious ERA-40 data, is that it has been constructed in a high horizontal resolution with a four dimensional variational analysis, it has an improved formulation of background error constraint, it was the result of a new humidity anal-ysis with improved model physics, it underwent a varia-tional bias correction using satellite radiance data and it included an improved fast radiative transfer model (Uppala et al. 2008). SSTs from ERA Interim fields were interpo-lated to the WRF model grid resolution and were also used as slowly varying lower boundary input. Surface topogra-phy data and 24 category land-use index data based on climatological averages, both at a 10′ and 30″ resolution, were obtained from the United States Geological Survey (USGS) database and were used for both the 27 and 9 km WRF domains.

Weather research and forecasting model was initialized using the 00 UTC 1 November data and was integrated up

to 00 UTC at the end of February for all the 20 DJF seasons (DJF 1991/1992 to DJF 2010/2011) considered in this study. The additional 1 month simulation (November) served as a model spin up, following the finding that a 1 month spin up period is sufficient for obtaining dynam-ical equilibrium between the lateral forcing and the internal physical dynamics of the model (Anthes et al. 1989). The model output data were saved in 6-h intervals.

Weather research and forecasting model results (from only the 9 km resolution domain) of the mean climatology as well as the interannual rainfall variability were compared to 0.5° gridded daily observational rainfall data obtained from the South African weather service (SAWS) rain gauge network. The rainfall station data that have been quality controlled by the Climate Services of the organization and interpolated to a regular grid of 0.5° × 0.5° resolution (Dyson 2009; Engelbrecht et al. 2013). The average rainfall amounts in each grid box are obtained using a weighted average. A rainfall station in any particular grid box which is geographically distant to other stations will have a larger weight factor and will therefore contribute more to the calculation of the average rainfall. Only grid boxes containing two or more rainfall stations (e.g. Engelbrecht et al. 2013) are used to produce the gridded rainfall data. The model simulated convective and stratiform rainfall are compared with respective TRMM 3A25 (Version 7) satellite derived monthly rainfall data available at 0.5° resolution. Large scale model simulated parameters are compared with ERA-interim data by interpolating the model data to ERA interim grid. The significance of the model simulated biases is calculated using Student's *t* test.

3 Spatial rainfall climatology and sources of model bias

3.1 Mean rainfall

The spatial distribution of the SAWS observed DJF rainfall averaged over the 20-year period (DJF 1991/1992–DJF 2010/2011; Fig. 2) shows most of the rainfall to be confined to east of South Africa, with KN, ML, LP, NW, GT, FS and east EC provinces experiencing rainfall ranging between 3 and 5 mm day^{-1} with maxi-mum rainfall between 5 and 8 mm day^{-1} over parts of Limpopo province. North Cape, West Cape and parts of East Cape provinces experience scanty rainfall during DJF season with less than 2 mm day^{-1} rainfall. It is interesting to note the large differences in the spatial distribution of rainfall simulated by the three cumulus parameterization schemes. In general, the WRF model succeeded in capturing the generally observed west-east

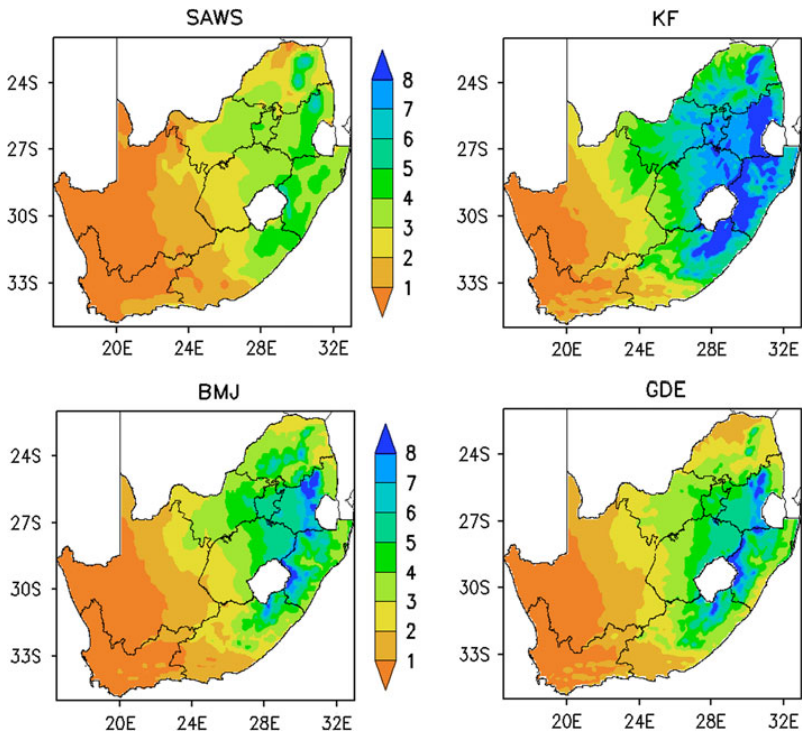

Fig. 2 Spatial patterns of mean rainfall climatology (mm day^{-1}) from 20-year December–January–February (DJF) simulations by the weather research and forecasting (WRF) model driven by the Kain–Fritsch (KF), Betts–Miller–Janjic(BMJ) and Grell–Devenyi ensemble (GDE) convective parameterization schemes. South Africa weather services (SAWS) observational rainfall data were used for verification

rainfall gradient over South Africa (Jury 2012). KF simulated mean rainfall exceeds 5 mm day^{-1} over the entire eastern South Africa with BM and GDE simulating rainfall comparable to SAWS observed rainfall. However, the rainfall over the western South Africa is well simulated by all the three cumulus schemes. Comparing the area averaged rainfall over the South Africa landmass simulated by KF (4.28 mm day^{-1}), BMJ (2.69 mm day^{-1}) and GDE (2.73 mm day^{-1}) with SAWS rainfall (2.11 mm day^{-1}), it is seen clearly that KF scheme overestimated the mean rainfall over South Africa during the DJF season with BMJ simulating closest to SAWS observed rainfall.

Overestimation of rainfall by the KF scheme is clearly brought out in Fig. 3 which shows the spatial distribution of significant biases in the rainfall simulation when com-pared with SAWS observed rainfall. KF simulated bias ranges from 1 mm day^{-1} in the West to 4 mm day^{-1} in the East. BMJ simulated significant biases are negative (about 1 mm day^{-1}) over the coastal region of Western Cape and Eastern Cape provinces of South Africa, while GDE sim-ulated dry biases over the north-eastern interior and some pockets of the east coast of South Africa. Nevertheless, wet or positive biases appear over most parts of the country in both the BMJ and GDE simulations though less in mag-nitude compared to KF simulated biases. All the three

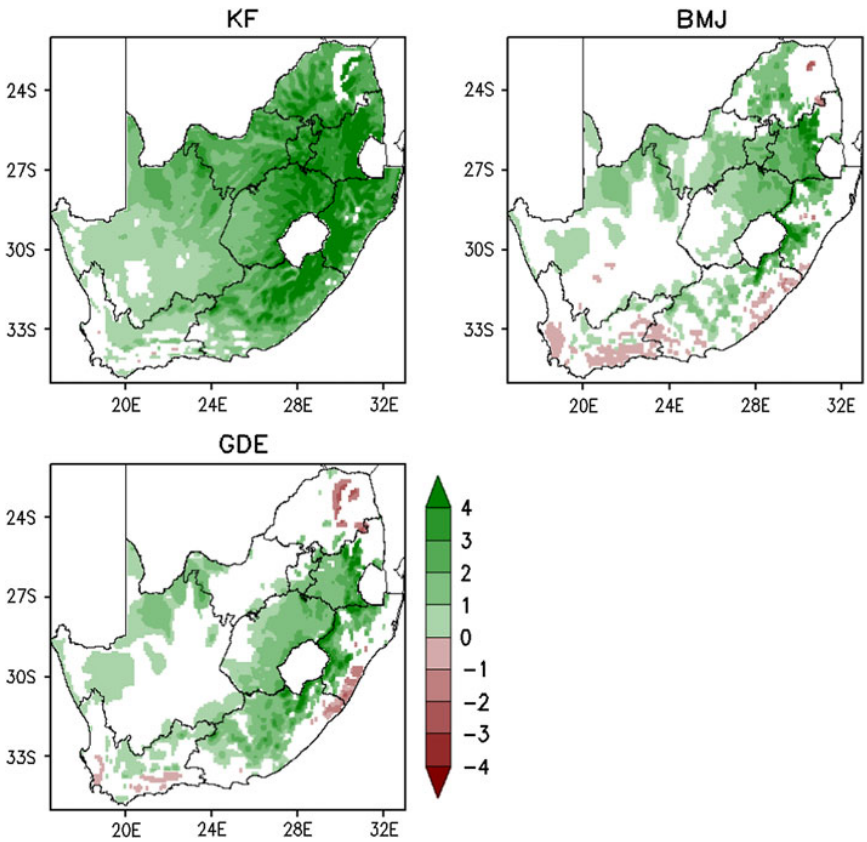

Fig. 3 Spatial patterns of mean rainfall climatology biases (mm day^{-1}) from the same simulations as defined in Fig. 2—relative to the South Africa weather services (SAWS) observational data. The *shaded* values are significant at the 99 % level using a student *t* test

Table 1 Quantitative mean rainfall climatology (mm day^{-1}) verifi-cation of spatial variability in 20-year weather research and forecast-ing (WRF) model simulations for December–January–February (DJF) driven by the Kain–Fritsch (KF), Betts–Miller–Janjic (BMJ) and Grell–Devenyi ensemble (GDE) convective parameterization schemes

	Spatial correlation coefficient (R)	Mean spatial bias	Mean absolute error (MAE)	Root mean square error (RMSE)
KF	0.91	2.17	2.18	2.77
BMJ	0.90	0.57	0.70	1.09
GDE	0.87	0.61	0.77	1.14

The South Africa weather services (SAWS) data serve as observations for verification

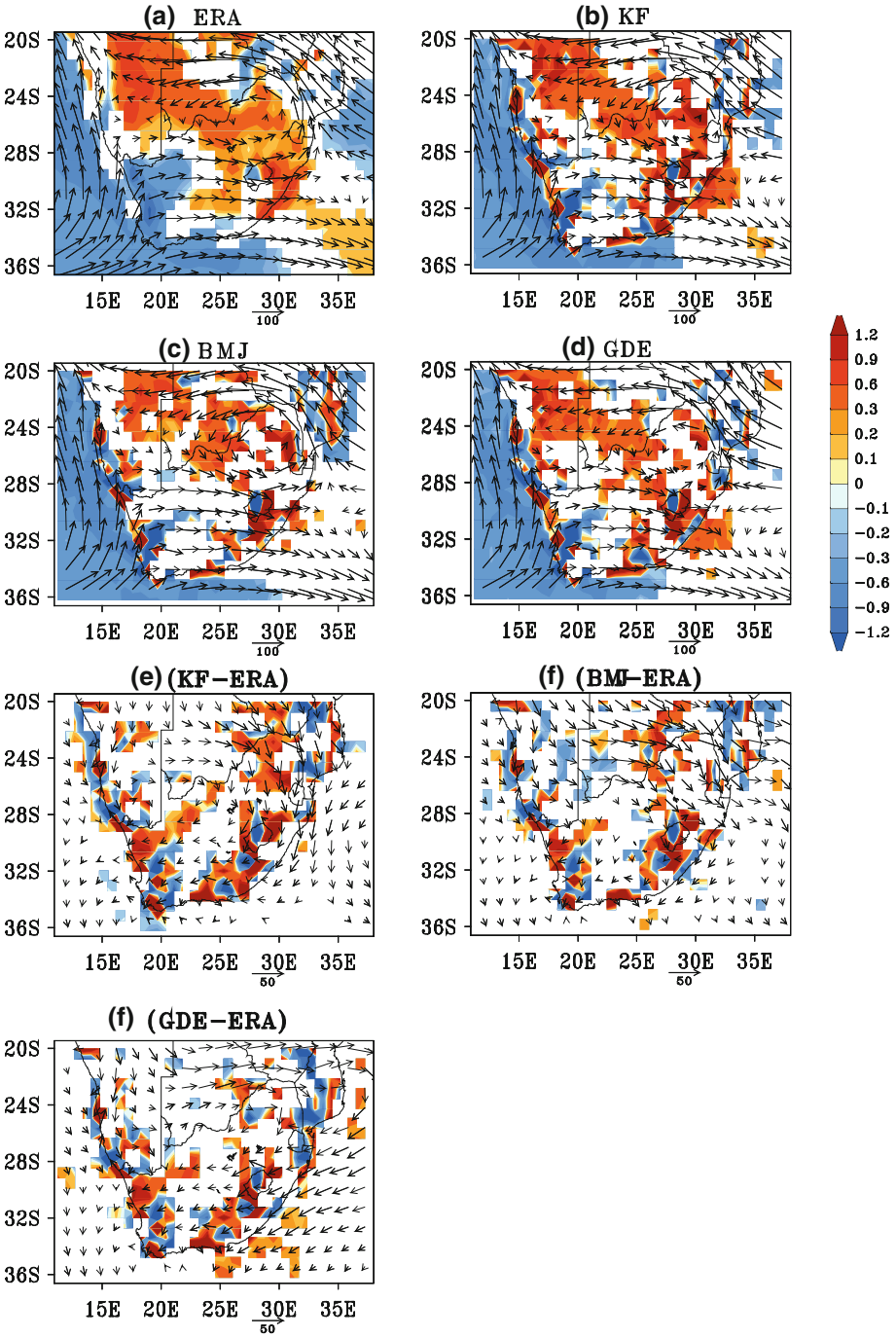

Fig. 4 Spatial patterns of the mean climatology of vertically integrated (from 1,000 to 300 hPa) moisture convergence and convergence biases (multiplied by $1 \times 10^{-4}\,s^{-1}$) (*shaded*) and moisture fluxes ($Kg\,m^{-1}\,s^{-1}$) (*arrows*) from the same simulations as defined in Fig. 2—Biases are calculated with respect to ERA interim data. The *shaded* values are significant at the 99 % level using a student *t* test

simulations show high wet biases near the Drakensberg Mountains, possibly related to a too strong topography effect on convection triggering.

To get a quantitative estimate of the biases simulated by the three cumulus parameterization schemes in the WRF model, we calculated the spatial correlation coefficient, mean spatial bias, mean absolute error (MAE) and root mean square error (RMSE) and the results presented in Table 1. From Table 1, it is seen that the simulated rainfalls for KF and BMJ convective parameterization schemes have high spatial correlations of R = 0.91 and R = 0.90, respectively, with SAWS observed rainfall. The GDE

simulated rainfall has a slightly less correlation coefficient of 0.87. Although the KF scheme has a high spatial correlation, it also has a significantly higher mean spatial bias (2.17 mm day^{-1}), high MAE (2.18 mm day^{-1}) and a high RMSE (2.77 mm day^{-1}), compared to the other two schemes (BMJ scheme: mean spatial bias = 0.57 mm day^{-1}, MAE = 0.70 mm day^{-1}, RMSE = 1.09 mm day^{-1}/GDE scheme: mean spatial bias = 0.61 mm day^{-1}, MAE = 0.77 mm day^{-1}, RMSE = 1.14 mm day^{-1}). Hence, the above analysis indicates that the BMJ convective parameterization scheme outperforms KF and GDE schemes in simulating the mean DJF rainfall over South Africa.

3.2 Thermodynamical characteristics

The above analysis shows quantitative differences in the performance of the three convection schemes in simulating the summer rainfall over South Africa. In this section we try to understand the causes of the differences in the performance by analyzing the moisture fluxes and various thermodynamic parameters simulated by the model. Analysis of rainfall distribution over South Africa due to the three cumulus parameterization schemes showed that, KF scheme has a tendency to simulate significant wet bias over all the provinces of South Africa. BMJ and GDE schemes also tend to simulate significantly higher rainfall over some provinces of South Africa with biases less than that simulated by KF scheme. However GDE scheme tends to simulate significantly less rainfall over parts of Limpopo province, the province vulnerable to droughts. To understand the causes of the differences in the rainfall simulated by the schemes, we plot significant biases in the vertically integrated (from 1,000 to 300 hPa) WRF model simulated moisture flux and its convergence. Vertical profiles of moisture, vertical velocity, temperature and equivalent potential temperature are also plotted. The biases are generated with respect to ERA interim data.

The mean, average of DJF 1991/1992 to DJF 2010/2011, vertically integrated moisture flux shows moisture being transported into southern Africa from the southwest Indian Ocean. Regions of significant moisture convergence are seen over parts of Namibia, Botswana and South Africa in the ERA Interim estimates and also in the model simulation with all the cumulus schemes (Fig. 4a–d). Moisture is also seen being transported into South Africa from the south

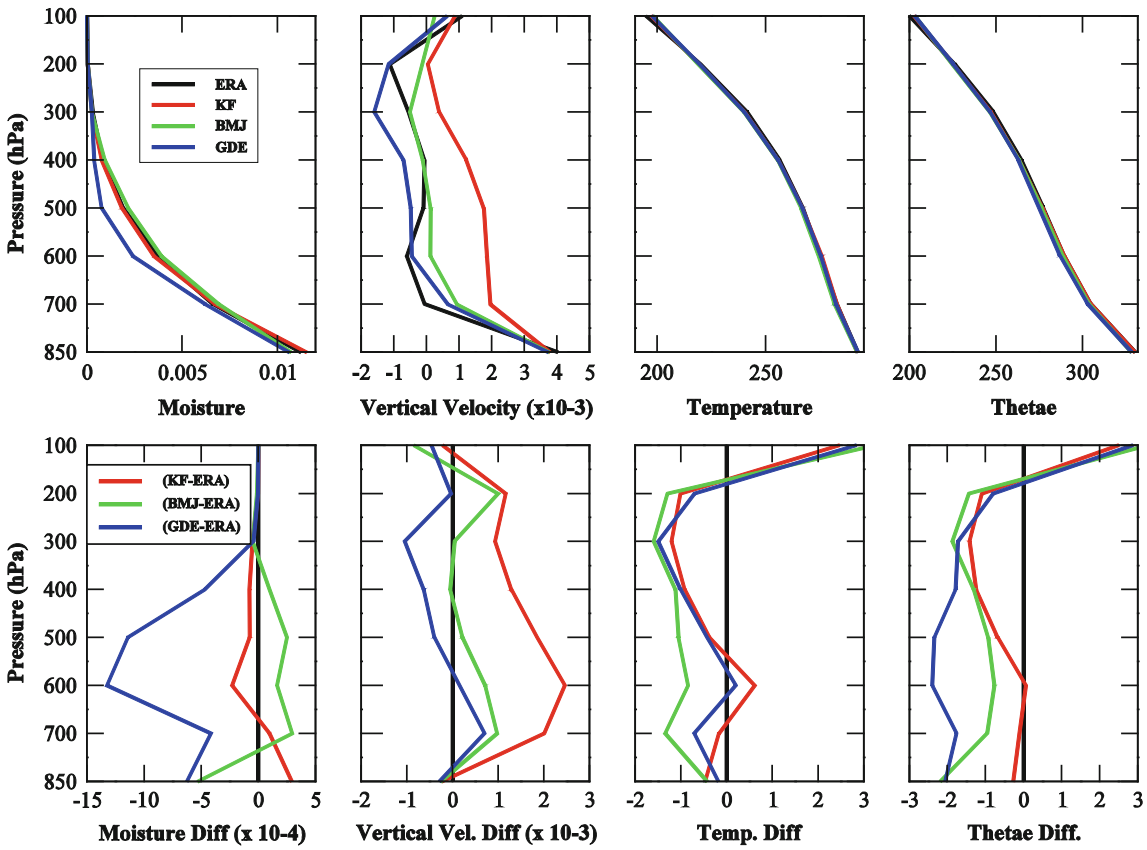

Fig. 5 Vertical profiles of area averaged mean (*top panel*) and biases (*bottom panel*) of moisture, vertical velocity, temperature and equivalent potential temperature over the Limpopo Province of South Africa from the same simulations as defined in Fig. 2. The bias is generated relative to ERA interim data

Atlantic Ocean. Regions of moisture divergence are seen over Zimbabwe and parts of Mozambique. Moisture divergence is also seen over the southwest Indian Ocean and south Atlantic Ocean in both the ERA Interim esti-mates and also in the model simulations. However, the three cumulus parameterization schemes show quantitative differences in both the moisture flux and its convergence. Mean biases in vertically integrated moisture from the KF scheme (Fig. 4e) with respect to the ERA Interim esti-mates, shows significant enhanced moisture being trans-ported into the entire South Africa from the tropics. Moisture flux convergence biases (shaded red in Fig. 4e) are also significantly higher compared to biases simulated by the BMJ scheme (Fig. 4f) and the GDE scheme (Fig. 4g), over the entire South Africa. The regions of positive biases in vertically integrated moisture conver-gence (Fig. 4) correspond well to the regions of positive rainfall biases (Fig. 3) simulated by the KF scheme. Ver-tically integrated moisture convergence simulated by the BMJ scheme (Fig. 4f) is positive over parts of South Africa. The moisture flux bias shows large flux being transported from the tropical regions into Limpopo, Mpumalanga and KwaZulu-Natal provinces (towards the north-eastern parts) of South Africa, creating areas of higher rainfall biases. However, unlike the KF simulated moisture flux bias, the moisture flux bias simulated by the BMJ scheme is seen transporting moisture out of the southern Africa landmass resulting in a lesser bias in moisture flux convergence compared to the KF simulation. The biases in the GDE simulated moisture fluxes (Fig. 4g) are directed towards the tropical regions and this generates negative biases in the moisture convergence over regions of southern Africa. However, the GDE scheme simulated moisture flux biases are directed towards South Africa from the South West Indian Ocean, creating regions of significant positive moisture convergence over the Mpumalanga, East Cape and Free State provinces. In general it is found that biases in the moisture fluxes and their convergence (divergence) as seen in Fig. 4 explain the biases in the spatial distribution of the rainfall.

To further find reasons for the rainfall biases over South Africa, vertical profiles of area averaged biases in moisture, vertical velocity, temperature and equivalent potential temperature were plotted over the Limpopo province, a region prone to droughts. Similar profiles were also pro-duced for the other eight provinces (Figures not shown). The vertical profiles of the mean moisture (Fig. 5 top panels) show GDE scheme underestimating moisture in the middle levels compared to the ERA Interim estimates. The KF and BMJ schemes simulated vertical moisture profile is comparable to the ERA Interim estimates. The vertical velocity is overestimated by the KF scheme compared to the ERA Interim estimates and underestimated by GDE scheme. All the schemes show decrease in temperature and equivalent potential temperature with height similar to the ERA Interim estimates. To understand the biases in the simulated precipitation we plot the biases in the above model simulated parameters with respect to the ERA Interim estimates (Fig. 5 bottom panels). Vertical profiles of biases in equivalent potential temperature give an indi-cation of the stability of the vertical atmospheric column simulated by the different convective schemes. The profile of equivalent potential temperature bias that becomes more negative with height indicates an unstable simulated profile than that of the observed, and vice versa (Gochis et al. 2002; Ratnam and Kumar 2005). Figure 5 depicts these area

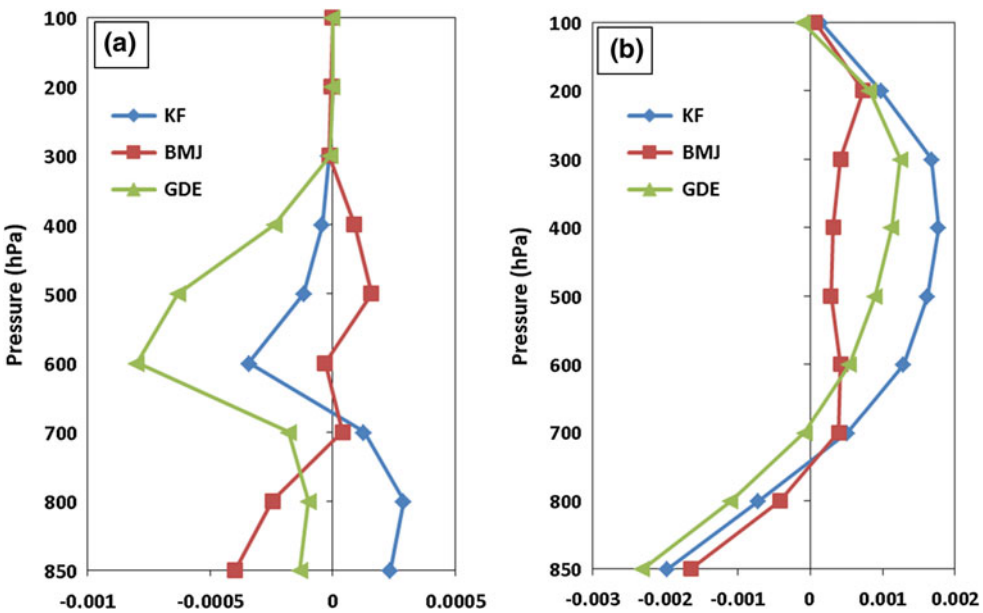

Fig. 6 Area averaged mean bias of (**a**) specific humidity (kg kg^{-1}) and (**b**) vertical velocity (m s^{-1}) over South Africa from the same simulations as defined in Fig. 2

average biases over the Limpopo province; the GDE scheme simulated moisture shows large negative bias throughout the troposphere, which is in agreement with the negative rainfall bias over Limpopo in the GDE simulation (Fig. 3) and the associated vertically integrated moisture flux biases in Fig. 4 that are mostly directed away from the South Africa in the GDE simulation. The profile of equivalent potential temperature biases indicates that the KF and BMJ schemes simulated a more unstable atmo-sphere in the mid-levels. The unstable atmosphere in the mid-level results from a positive bias in vertical velocities (Fig. 5). The unstable atmosphere simulated in the KF simulation can contribute to the large positive biases in rainfall over the Limpopo region (Fig. 3). The negative bias in moisture, along with a stable atmosphere and neg-ative biases of vertical velocity simulated by GDE resulted in the predominantly negative rainfall bias (Fig. 3) over the Limpopo province. In general vertical profiles of atmospheric variables over all other provinces (Figures not shown) also provide a good explanation for the associated rainfall biases depicted in Fig. 3.

Convective parameterization schemes in atmospheric models generate rainfall according to the availability of moisture and the stability/instability of the atmosphere, which in turn, could affect the general simulation of seasonal circulation. It is, therefore, important to understand the liquid water content and the thermodynamic structure of the atmosphere under consideration. The vertical profile of the mean bias of domain averaged specific humidity (kg kg^{-1}) and vertical velocity (m s^{-1}) over South Africa is presented in Fig. 6. Model simulated fields were interpolated to ERA interim data fields from where the area averaged bias was calculated. Figure 6 illustrates wetter low-level conditions (up to 700 hPa) with dryer mid-level conditions (600–500 hPa) returning to normal at higher levels for the KF scheme, dry low level conditions with wetter mid to high level conditions for the BMJ scheme, and dry to very dry conditions from low to mid-levels returning to normal at higher levels for the GDE scheme. The profiles of vertical velocity in Fig. 6 shows that all simulations overestimated these velocities compared to observations, where the KF scheme had a maximum bias with strong upward motion from the 700 to 200 hPa level, compared to the BMJ and GDE schemes. The BMJ scheme appears to be close to what had been observed. The moist atmosphere and strong upward motion in the KF scheme proof to be the result of a moister unstable atmosphere, from where the largest positive bias in seasonal rainfall (Fig. 3) developed.

To establish convective instability in the three convective parameterization schemes, mean CAPE values were calculated, and are presented in Fig. 7. ERA interim estimated CAPE has values between 300 and 400 J/Kg over Botswana and parts of South Africa and values between

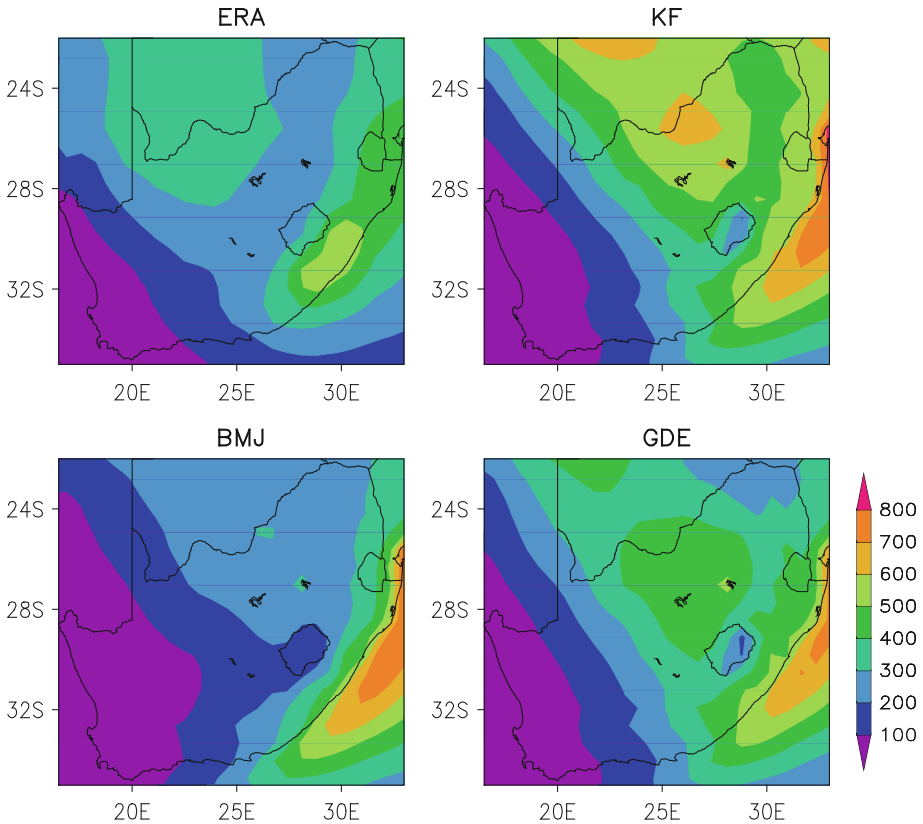

Fig. 7 ERA interim estimated and model simulated December–January–February (DJF) mean climatology of convective available potential energy (CAPE) (J kg^{-1}), as compared to the Kain–Fritsch (KF), Betts–Miller–Janjic (BMJ) and Grell–Devenyi ensemble (GDE) convective parameterization scheme experiments

400 and 500 J/Kg over the eastern parts of South Africa with a peak over KN and EC provinces. KF scheme generated the highest level of instability, which seems to produce a highly convective unstable atmosphere and that triggered the simulation of the largest positive rainfall biases over South Africa (Fig. 3). Between the BMJ and GDE schemes, the GDE scheme has a more convective unstable environment, which also explains its relatively high positive rainfall bias (Fig. 3). As a matter of fact the KF and GDE schemes generated more convective rainfall compared to stratiform rainfall (Fig. 8). The smallest CAPE values in the BMJ scheme (Fig. 7) generated less convective rainfall (Fig. 8) compared to the KF and GDE schemes. As satellite derived rainfall from the tropical rainfall measuring mission (TRMM) became available from December 1997, the TRMM observed convective and stratiform rainfall was compared to the associated model simulations over a 14-year DJF period (1997/1998–2010/2011) (Fig. 9). Rainfall observations show that convective rainfall is higher than stratiform rainfall over South Africa during this 14-year period. Although the combined (convective and stratiform) mean rainfall simulated by the BMJ scheme is closer to observe, there are a difference in performance if the two components of rainfall are separately compared to observations. It can be clearly seen from Fig. 9 that the convective and stratiform rainfall simulated with BMJ scheme was close to the TRMM estimates. The KF and GDE scheme overestimated the convective rain and underestimated the stratiform rain.

4 Interannual variability

Southern Africa is often regarded as being a predominantly semiarid region with a high degree of interannual rainfall variability (Richard et al. 2000; Reason et al. 2000;

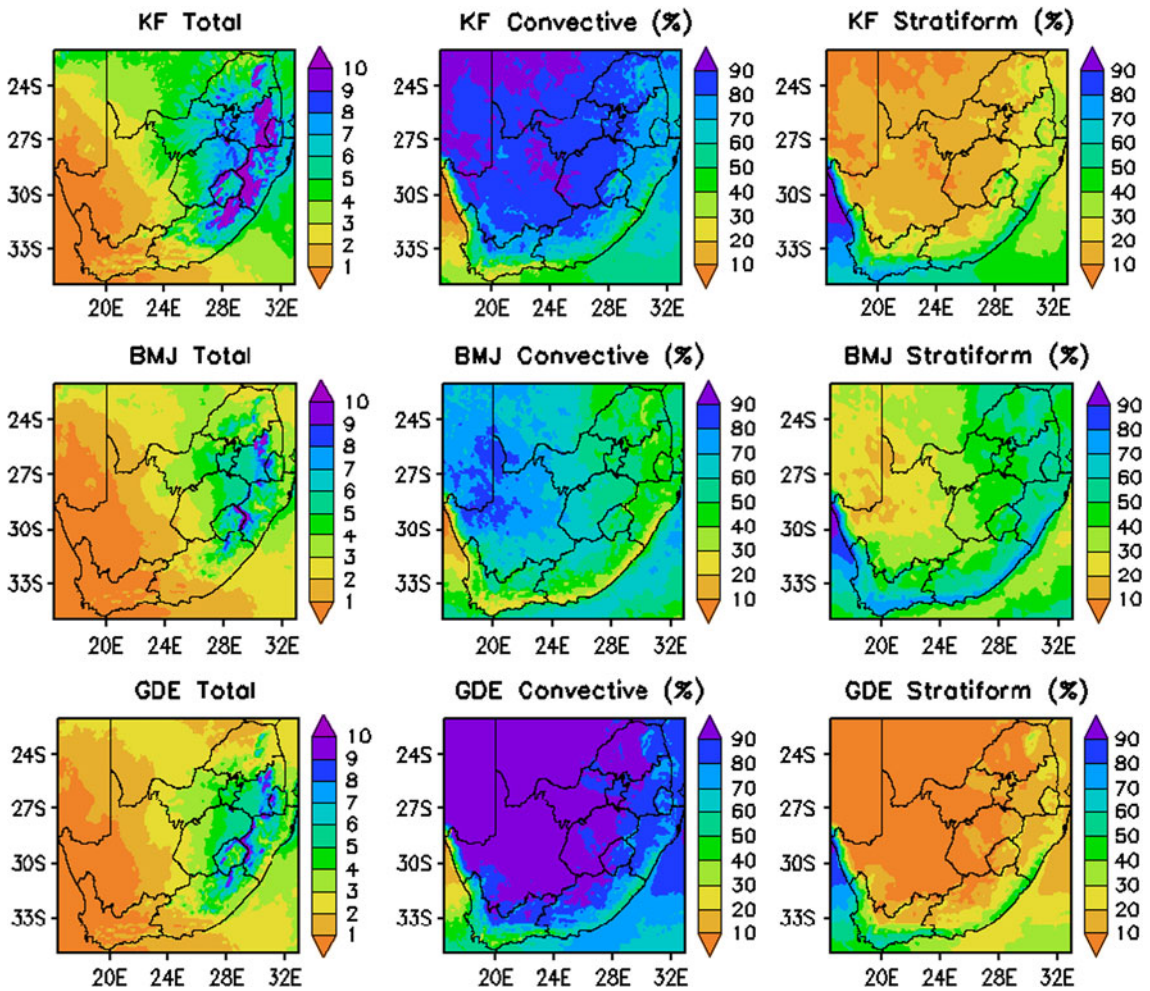

Fig. 8 Model simulated DJF mean climatology (1991/1992–2010/2011) of total rainfall (mm/day, *left panel*), convective rainfall (%, *middle panel*) and stratiform rainfall (%, *right panel*)

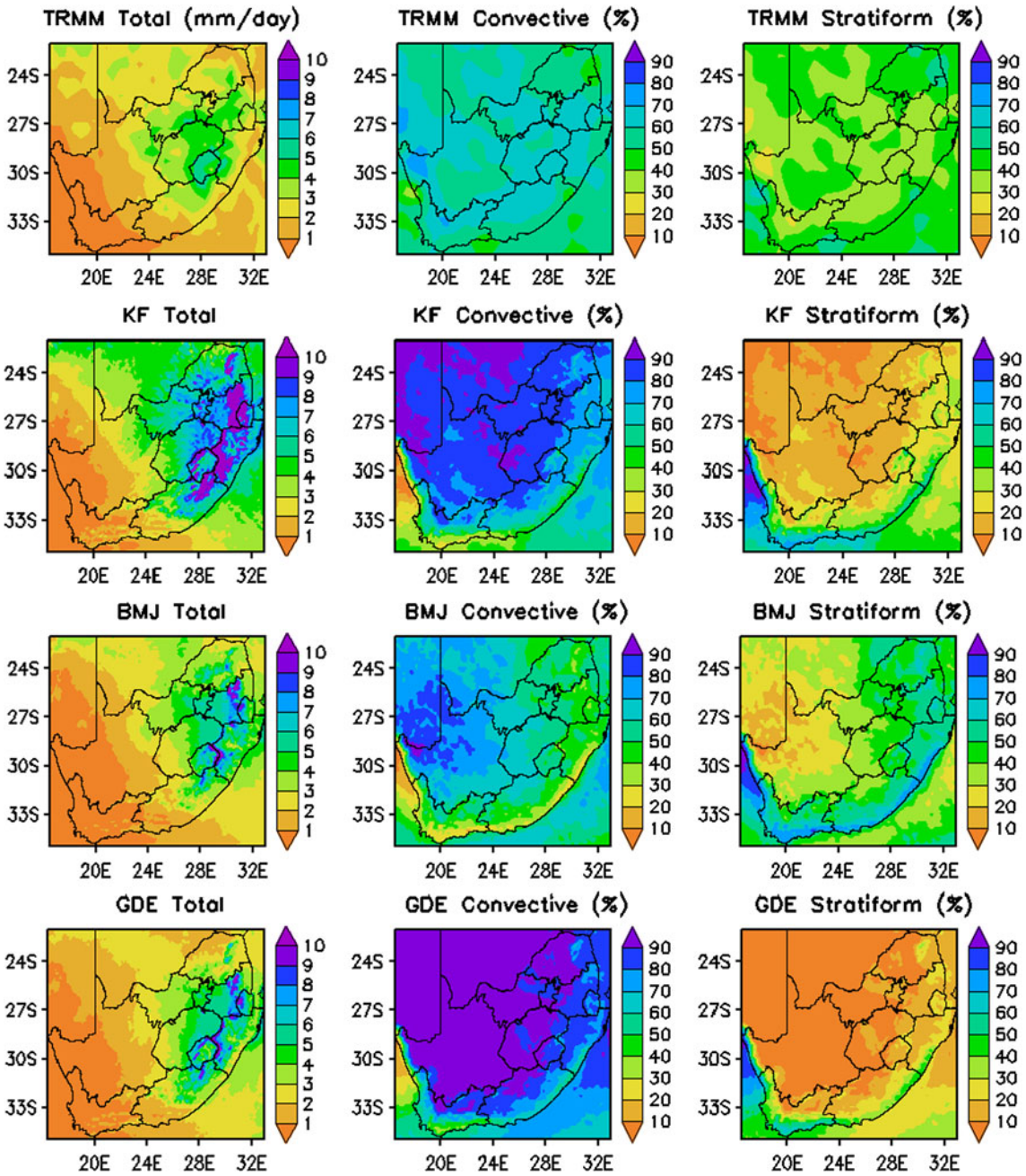

Fig. 9 December–January–February (DJF) mean climatology (1997/ 1998–2010/2011) of total rainfall (mm/day), convective rainfall (%) and stratiform rainfall (%) from the Kain–Fritsch (KF), Betts–Miller–Janjic (BMJ) and Grell–Devenyi ensemble (GDE) convective parameterization schemes—compared to the TRMM estimates

Washington and Preston 2006; Fauchereau et al. 2009). In any attempt to employ a RCM for short and longer-term prediction, it is important to determine if the RCM is capable of capturing the observed interannual variability. In this section we investigated if the WRF model can realistically capture the interannual variability in the simulated rainfall over the study period. The model simulated summer rainfall anomalies for each of the three schemes calculated from its own climatology.

Figure 10 illustrates the standardized anomaly of area averaged model simulated rainfall over South African continental grid points from the 20-year DJF simulations by the WRF model driven by the KF, BMJ and GDE convective parameterization schemes, as compared to SAWS observations. The Coefficient of Variability (CV = [standard deviation/mean] $\times$ 100) in SAWS rain-fall observations over the 20-year study period is found to be 28.27 %. The associated CVs in WRF model

simulations driven by the KF, BMJ and GDE convective parameterization schemes were 20.99, 21.28 and 21.94 %, respectively, indicating a lower degree of variability in model simulated rainfall which are relatively close to each other, compared to observations. In order to find the cumulus parameterization scheme closest to observed variability, correlation coefficients were calculated between model simulated and observed seasonal anomalies for the 20 year period. The BMJ with a high correlation ($R = 0.81$) with the SAWS observed rainfall outperforms the KF ($R = 0.73$) and GDE ($R = 0.64$) schemes in the simulation of the variability of rainfall anomalies over South Africa during the austral summer season.

4.1 ENSO response

The interannual variability of rainfall over southern Africa is dominated by the influence of ENSO (Lindesay 1988; Reason et al. 2000; Cook 2000, 2001; Reason and Rouault 2002; Richard et al. 2000, 2001; Misra 2003; Rouault and Richard 2005; Reason and Jagadheesha 2005; Washington and Preston 2006; Cre´tat et al. 2010 and Ratna et al. 2013 among others). ENSO effects on southern Africa rainfall are non-linear with wet (dry) anomalies during La Nin˜a (El Nin˜o) years. The physical mechanism through which ENSO influences southern Africa climate variability is reported some of the earlier study. Ratna et al. (2013) reported that low level divergence (convergence) is observed over southern Africa due to change in the Walker circulation during El Nin˜o (La Nin˜a) events. The anomalous lower level divergence over the landmass during El Nin˜o season prevents maritime moisture transport to southern Africa, thereby reducing the number of synoptic disturbances and the seasonal rainfall. Ratna et al. (2013) also found that during La Nin˜a (El Nin˜o), there is an anomalous high (low) just south of South Africa and this anomalous anticyclonic (cyclonic) circulation favors (disfavors) mid-latitude winds flow towards continental southern Africa and hence causes enhanced (reduced) rainfall. Cook (2001) indicated that in the Southern Hemisphere ENSO generates atmospheric Rossby waves, which could be responsible for an eastward shift of the convergence zone where most of the synoptic scale rains bearing systems like TTTs occur. However, Nicholson and Kim (1997) suggested that the SST anomalies over the India Ocean could shift atmospheric convection and rain-fall eastward during El Nin˜o events.

The correlation coefficient between observed rainfall over South Africa and Nino3.4 SSTs over the 20-year DJF period is -0.57. The correlation between simulated rainfall and the Nino3.4 is -0.66, -0.69 and -0.49 for the KF, BMJ and GDE convective parameterization schemes, respectively. In order to investigate the influence of ENSO on WRF simulated seasonal rainfall, results from Fig. 10 were further classified into dry, normal and wet categories. The normalized SAWS rainfall anomaly (Fig. 10) also helps in identifying extreme wet and dry years in the study period. If we take extremely wet (dry) year to be the year with normalized rainfall to be greater (less) than 1 (-1), then we find four (three) extreme wet (dry) years in the 20 year period considered in the study. Interestingly, all the observed very dry years correspond to El Nino years and very wet years correspond to the La Nina years. Observed and model simulated dry, normal and wet DJF rainfall seasons, as compared to the corresponding El Ni˜no, neutral and La Nin˜a episodes are given in Table 2.

In observations (SAWS in Table 2), three seasons were identified as being dry—1991/1992, 1994/1995 and 2006/2007 associated with El Nin˜o conditions in the Pacific. All convective parameterization schemes generated

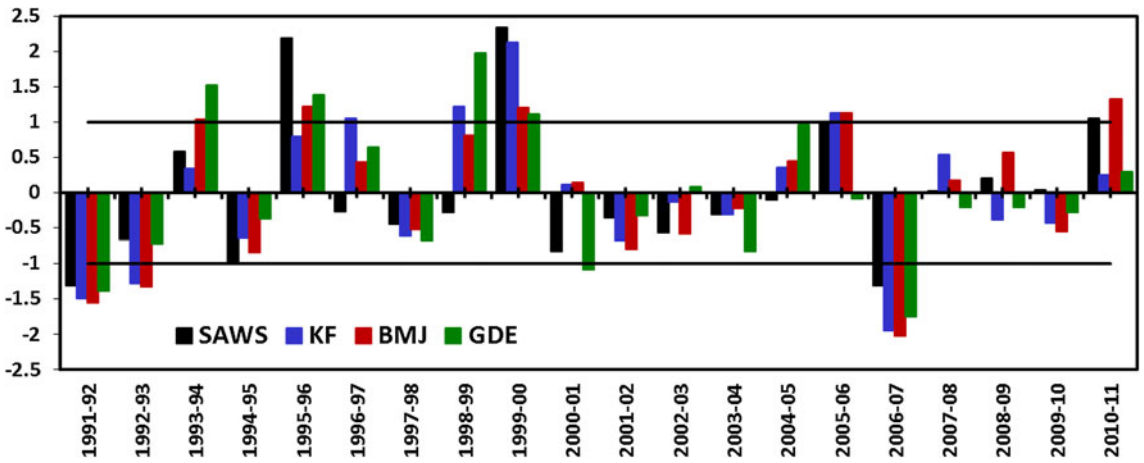

Fig. 10 Standardized rainfall anomalies for the South African domain from the same simulations as defined in Fig. 2, relative to the South African weather service (SAWS) observational data. The ±1 standardized anomaly values are indicated by solid black lines in order to define dry (\-1), normal (between -1 and ?1) and wet ([?1) rainfall categories

Table 2 Observed and model simulated dry, normal and wet rainfall seasons (as defined in Fig. 10), compared to El Nin˜o, neutral and La Nin˜a events

		El Niño	Neutral	La Niña
Dry	SAWS	1991/1992, 1994/1995, 2006/2007		
	KF	1991/1992, 2006/2007	1992/1993	
	BMJ	1991/1992, 2006/2007	1992/1993	
	GDE	1991/1992, 2006/2007		2000/2001
Normal	SAWS	1997/1998, 2002/2003, 2004/2005, 2009/2010	1992/1993, 1993/1994, 1996/1997, 2001/2002, 2003/2004, 2008/2009	1998/1999, 2000/2001, 2007/2008
	KF	1994/1995, 1997/1998, 2002/2003, 2004/2005, 2009/2010	1993/94, 2001/2002, 2003/2004, 2008/2009	1995/1996, 2000/2001, 2007/2008, 2010/2011
	BMJ	1994/1995, 1997/1998, 2002/2003, 2004/2005, 2009/2010	1996/1997, 2001/2002, 2003/2004, 2008/2009	1998/1999, 2000/2001, 2007/2008, 2010/2011
	GDE	1994/1995, 1997/1998, 2002/2003, 2004/2005, 2009/2010	1992/1993, 1996/1997, 2001/2002, 2003/2004, 2005/2006, 2008/2009	2007/2008, 2010/2011
Wet	SAWS		2005/2006	1995/1996, 1999/2000, 2010/2011
	KF		1996/1997, 2005/2006	1998/1999, 1999/2000
	BMJ		1993/1994, 2005/2006	1995/1996, 1999/2000
	GDE		1993/1994	1995/1996, 1998/1999, 1999/2000

dry conditions for the seasons 1991/1992 and 2006/2007, although the model simulated dry is stronger in magnitude. Although still negative, all schemes failed in reproducing the extreme dry conditions experienced in 1994/1995. The BMJ scheme was the closest to observations though it couldn't simulate the drought.

Of the four extreme wet years, DJF 1995/1996, 1999/1900, 2005/2006 and 2010/2011, except DJF 2005/2006 all the years are associated with La Nin˜a events in the Pacific. DJF of 2005/2006 was associated with the weaker La Nin˜a type of cooling in the central Pacific but there was a positive sub-tropical IOD (Behera and Yamagata 2001) with positive SST anomalies near the east coast of southern Africa and negative SST anomalies near the west coast of Australia. A positive subtropical dipole helps moisture transports from the Indian Ocean to southern Africa. From Fig. 10 it can be seen that all the convective schemes get correct sign of the rainfall anomalies though they simulate less amplitude rainfall anomalies compared to the SAWS normalized rainfall anomalies. All convective parameterization simulations generated wet conditions for the two seasons 1995/1996 and 1999/1900, although rainfall totals were less than observed. For the 2005/2006 season both the KF and BMJ schemes yielded wet conditions, while the GDE could not generate wet conditions. For the 2010/2011 season, the KF and GDE schemes fail to generate wet conditions, while the BMJ scheme generated wet conditions. In general, the BMJ scheme was superior to the other two schemes in generating wet conditions, but like the other schemes, could not capture the observed extreme values in magnitude.

A total of 13 observed summer seasons fell in the normal category. Amongst these seasons, 1998/1999, 2000/2001 and 2007/2008 were associated with La Nin˜a conditions. For the La Nin˜a year 1998/1999, all the schemes simulated wet to near-wet rainfall. In the year 2007/2008, all schemes generated normal rainfall conditions. Surprisingly, even though 2000/2001 was a La Nin˜a year, near drought conditions were observed over South Africa. Though the performance of GDE scheme is poor for most of the year, this scheme could simulate the dry condition over South Africa for the year 2000/2001. Similarly, the year 1997/1998, 2002/2003, 2004/2005 and 2009/2010 were associated with El Nin˜o conditions but South Africa experienced normal rainfall. Even though the 1997/1998 is known to be strongest El Nin˜o of the year, South Africa hasn't experienced a severe drought though the seasonal rainfall was below normal. All the three schemes could successfully simulate the below normal seasonal rainfall. All the simulations could simulate the normal rainfall over South Africa for 2002/2003, 2004/2005 and 2009/2010.

The above analysis shows that the regional model responds well to the major climatic forcings such as ENSO and subtropical IOD with BMJ performing the best in simulating the interannual variability.

4.2 Dry and wet seasons

To look at the reasons for the model's performance in simulating the rainfall anomalies of amplitudes comparable

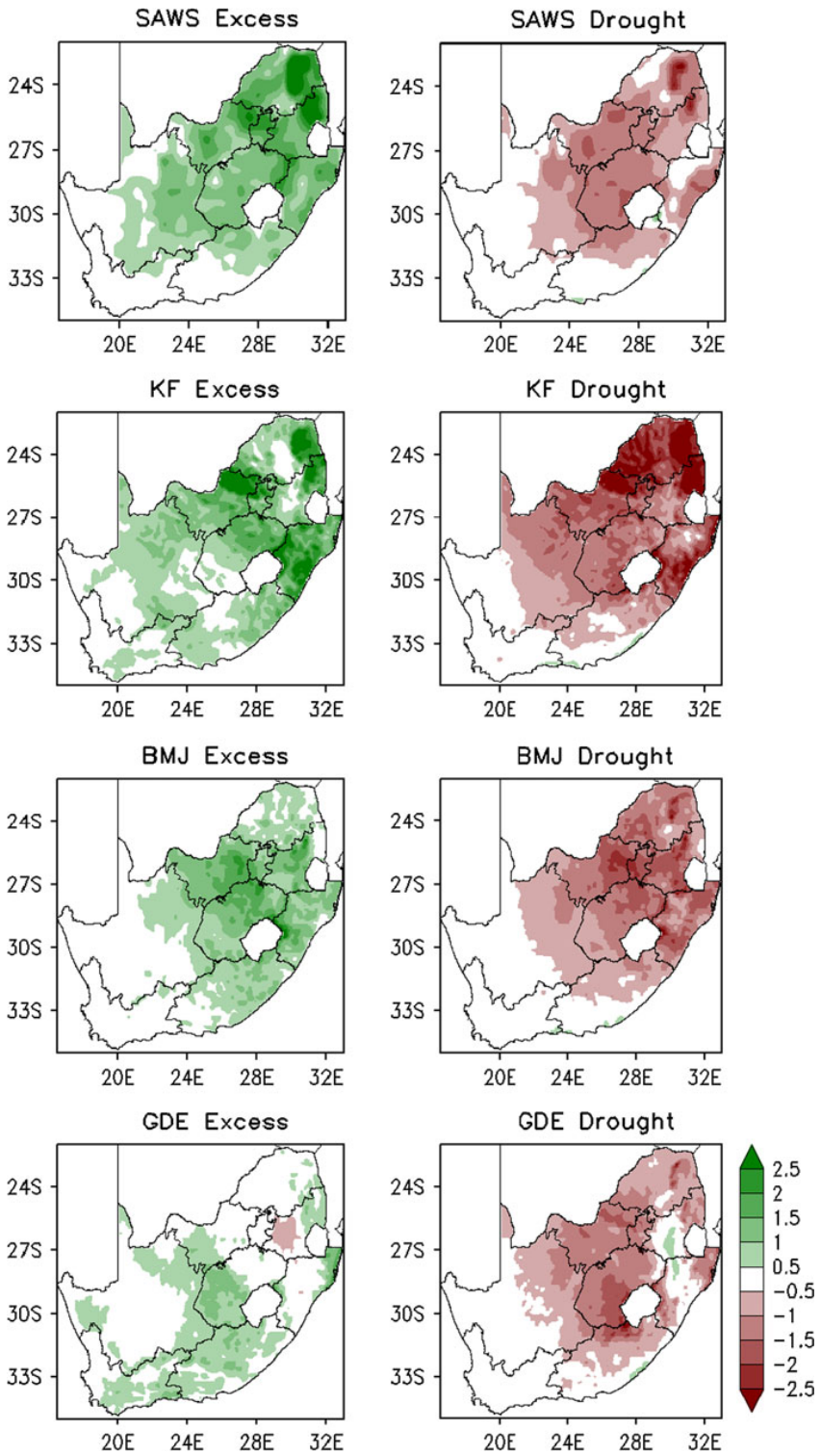

Fig. 11 Composite anomalies of observed and model simulated rainfall during three dry seasons (1991/1992, 1994/1995, and 2006/2007) (*right*) and four wet seasons (1995/1996, 1999/2000, 2005/2006 and 2010/2011) (*left*) from the same simulations as defined in Fig. 2 and South Africa weather service (SAWS) observational data

to SAWS rainfall anomalies, we composited the rainfall of the four extreme wet seasons (1995/1996, 1999/2000, 2005/2006 and 2010/2011) and three dry seasons (1991/1992, 1994/1995, and 2006/2007) for the SAWS observed anomalies and the model simulated anomalies and presented in Fig. 11.

Observed anomaly during the wet (dry) season (Fig. 11) shows that the rainfall is above (below) normal over most parts of the country. Rainfall is very high (low) over the east Limpopo and north Mpumalanga provinces compared to the other regions during the wet (dry) seasons. All the three cumulus schemes could simulate the excess and deficient rainfall over the country similar to the SAWS observed anomalies but with variations in intensity and location. The spatial distribution of the KF simulated rainfall shows three peaks in rainfall over eastern Limpopo, northeast region of Northwest province and Kwazulu-Natal during the excess rainfall season. These regions also correspond to deficient rainfall during the extreme dry seasons. The intensity of high (low) rainfall during the wet (dry) years in the KF simulation is high compared to the SAWS observed rainfall anomalies (Fig. 11). The spatial pattern of BMJ simulated rainfall during the very wet season shows weaker rainfall anomalies compared to

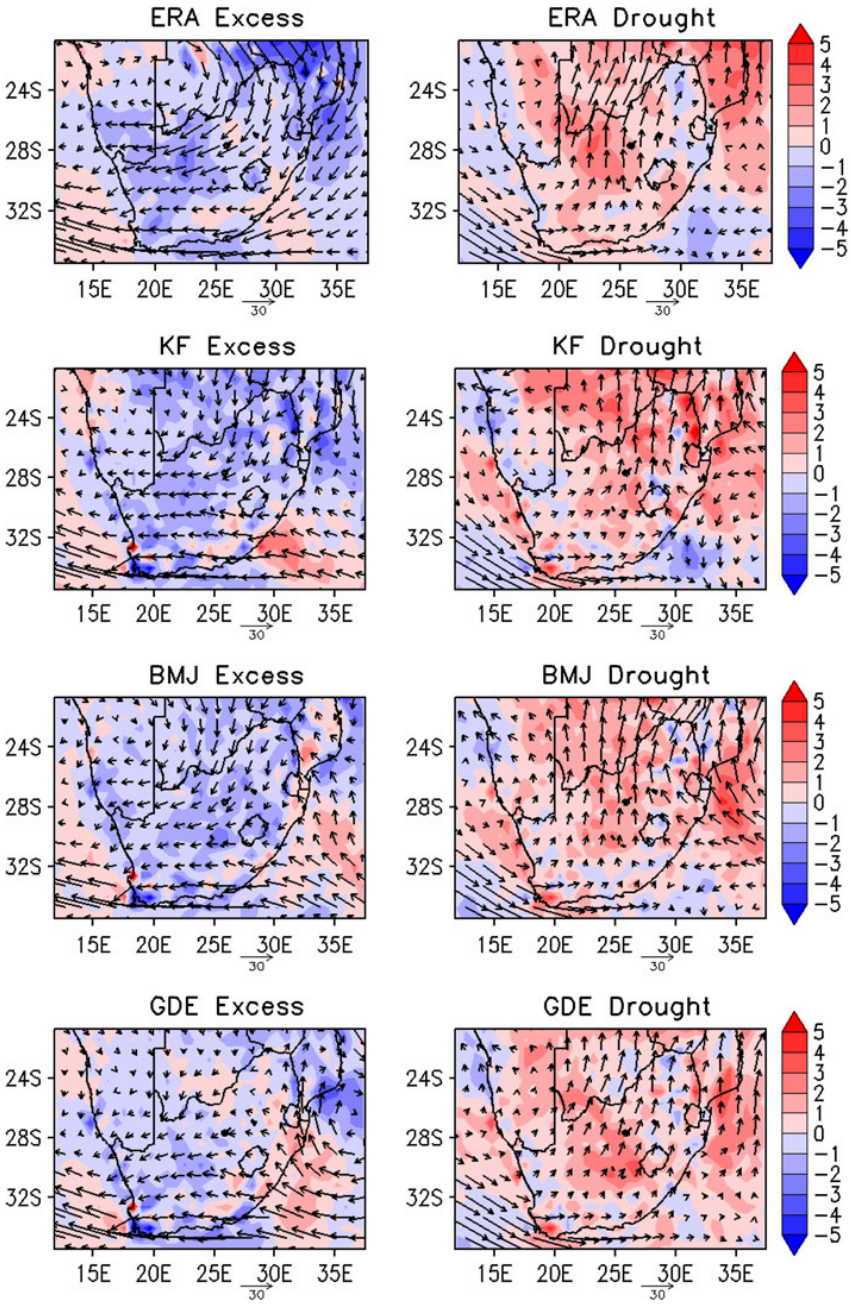

Fig. 12 Composite dry (*right*) and wet (*left*) season patterns of anomalies in vertically integrated (from 1,000 to 300 hPa) moisture divergence (multiplied by $1 \times 10^5\ s^{-1}$) (*shaded*) and moisture fluxes ($kg\ kg^{-1}\ M\ s^{-1}$) (*arrows*) from the same simulations as defined in Fig. 2—relative to ERA interim data. The *shaded* values are significant at the 99 % level using a student t test

SAWS observed anomalies. However, the rainfall anomalies simulated by BMJ during dry years agree well with the SAWS observed anomalies. GDE scheme on the other hand had problems in simulating both the wet and dry conditions.

In order to find a reason for the composite dry and wet anomalies in Fig. 11, composite anomalies of vertically integrated moisture divergence and fluxes were calculated from WRF simulated and ERA interim data (Fig. 12). During very high rainfall years anomalous convergence of moisture is seen throughout South Africa except over parts of East Cape, with moisture anomalies being transported cyclonically from the tropical regions (Fig. 12). During dry years, anomalous divergence is seen over most parts of South Africa with moisture being transported from the subtropical south Atlantic towards the tropics. The anomalous convergence over South Africa in the KF and BMJ is weaker than ERA-Interim estimated convergence. Also, the anomalous transfer of moisture into South Africa is weaker compared to ERA-Interim estimates, resulting in weaker than observed rainfall anomalies during the observed very high rainfall years. However, during drought years anomalous divergence is stronger than ERA-interim estimates in both the KF and BMJ simulations results in intense droughts compared to SAWS observed droughts. GDE scheme on the other hand simulated weak transport into South Africa during excess rainfall years and also weak divergence during drought years showing the limi-tations in using GDE scheme over South Africa for simu-lating seasonal rainfall during austral summer months.

5 Provincial rainfall variability

Figure 2 shows that there is a high degree of spatial variation in rainfall across South Africa. In order to verify the WRF model performance at smaller spatial scales the interannual variability of standardized mean seasonal rainfall anomalies, relative to the 20-year study period's climatology, were calculated over the nine provinces of South Africa (see Fig. 1) and presented in Fig. 13.

Apart from the area averaged (or means) illustrated in Fig. 13, the mean, CV and the correlation coefficient between the simulated and observed anomalies are calculated and shown in Table 3.

In accordance with the climatology of the South Africa rainfall (Fig. 2), the eastern provinces receive higher rainfall compared to the western provinces. Observed provincial mean seasonal rainfall values (Table 3) over the east are: Kwazulu-Natal (3.97 mm day^{-1}), followed by Mpumalanga (3.88 mm day^{-1}) and Gauteng (3.76 mm day^{-1}). Note that these three provinces are located across the eastern escarpment mountains, where the KwaZulu-Natal Province is on the windward side of the mountain ranges. Drier provinces are: Limpopo (2.92 mm day^{-1}), the Free State (2.91 mm day^{-1}) and North-West (2.79 mm day^{-1}). The most western province is the Western Cape (0.67 mm day^{-1}), which receives very little rain during the austral summer.

With the exception of the Limpopo province, mean area averaged rainfall is generally overestimated by all there convective parameterization schemes (Table 3), which is consistent with the rainfall biases over South Africa (Fig. 3). CVs in Table 3 indicating that the observed interannual variability is highest over the Northern Cape province, and the lowest over the Eastern Cape province. Amongst the provinces that has the highest mean observed rainfall (mostly over the east), Limpopo province experience the highest rainfall variability (according to the CV in Table 3). It can be seen from Table 3 that the magnitude of interannual variability is generally underestimated by all the WRF convective parameterization schemes—except for the Western Cape Province.

To check the relationship between the model and observed rainfall, we calculated the correlation coefficient between two series of data. The GDE scheme has the lowest correlation coefficients with observations for all provinces although it's simulated CV is slightly closer to the observed CV. The correlation coefficient of the BMJ simulated rainfall with SAWS rainfall over the provinces shows high values for most of the provinces, except for the Limpopo and KwaZulu-Natal provinces. The rainfall sim-ulated by KF shows the higher correlation coefficient only for the two provinces but the CV is low compared to the BMJ and GDE schemes. Note that all the schemes failed to reproduce the observed interannual variability over the Limpopo Province. Interannual variability by the BMJ scheme was better than that of the KF and GDE schemes for most of the provinces, as reflected in the high CC and CV values (Table 3). Rainfall biases are also listed in Table 3, which correspond well with the standardized anomalies (Fig. 13). Overall, Fig. 13 and Table 3 both indicate that, except for a few cases where the GDE scheme performed better, the BMJ scheme performed the best in capturing the observed anomalies/biases, as well as the magnitude of interannual variability.

6 Rainy days and rainfall categories

As discussed in previous sections, KF scheme overestimates the rainfall over South Africa during the austral summer and the GDE underestimates rainfall. Rainfall simulation by BMJ scheme outscores both the KF and GDE scores. In this section we further analyze the performance of the schemes in simulating the rainfall over South Africa in terms of the

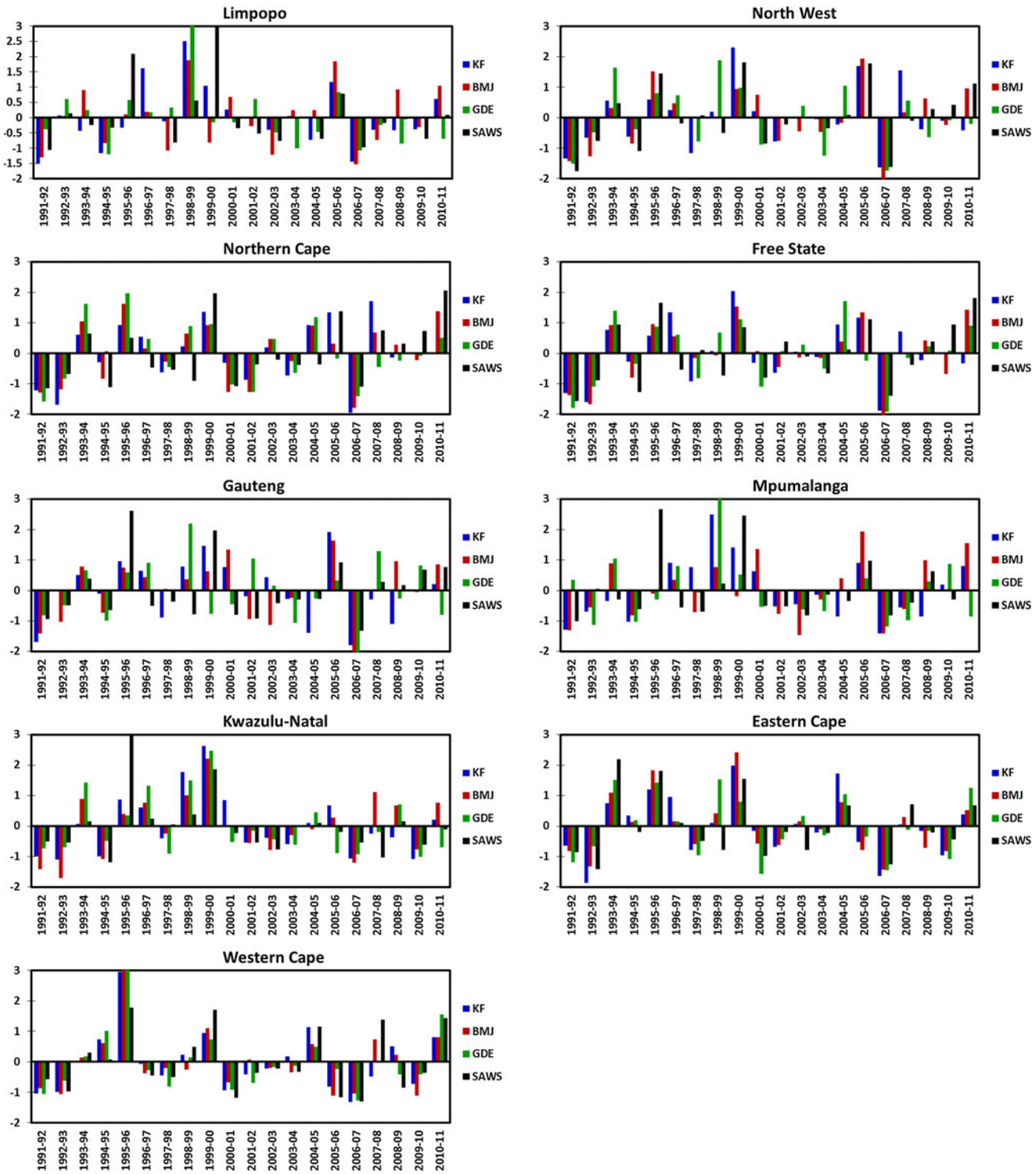

Fig. 13 Interannual variability of standardized area averaged mean seasonal rainfall anomalies for each of the nine South African provinces from the same simulations as defined in Fig. 2—relative to the South Africa weather service (SAWS) observational data

number of rain days and in terms of the various categories of rainfall based on rainfall intensity. The term "rainy days" refer to a day on which the amount of rainfall recorded or simulated at any grid point was more than 1 mm.

It was firstly noted from SAWS observations (Fig. 14) that a high spatial variability in number of rainy days occurred during the summer rainfall season. The eastern parts of South Africa experienced the maximum number of

Table 3 Mean, coefficient of variability (CV), correlation coefficient and bias of the inter-annual variability in standardized area averaged mean seasonal rainfall anomalies for each of the nine South African provinces from the same simulations as defined in Fig. 2, relative to the South Africa weather service (SAWS) observational data

		SAWS	KF	BMJ	GDE
LP	Mean	2.92	5.57	3.68	2.70
	CV	43.71	33.77	29.10	36.79
	CC		0.50	0.28	0.29
	Bias		2.64	0.76	−0.23
NW	Mean	2.79	5.39	3.61	3.26
	CV	30.11	29.36	27.61	31.12
	CC		0.71	0.84	0.50
	Bias		2.60	0.82	0.47
NC	Mean	0.84	1.89	1.12	1.24
	CV	51.09	36.32	30.38	40.91
	CC		0.63	0.69	0.45
	Bias		1.05	0.28	0.40
FS	Mean	2.91	5.86	3.74	4.13
	CV	31.03	21.03	24.63	23.89
	CC		0.50	0.77	0.67
	Bias		2.96	0.84	1.22
GT	Mean	3.76	7.34	5.18	4.67
	CV	30.52	19.95	24.01	20.47
	CC		0.55	0.57	0.15
	Bias		3.58	1.42	0.91
ML	Mean	3.88	8.14	5.72	5.42
	CV	31.39	19.56	22.00	14.54
	CC		0.38	0.31	0.17
	Bias		4.26	1.83	1.54
KN	Mean	3.97	8.27	5.04	5.15
	CV	27.58	21.71	23.26	19.74
	CC		0.66	0.52	0.54
	Bias		4.29	1.07	1.18
EC	Mean	2.39	4.85	2.65	3.28
	CV	23.29	19.69	25.31	23.48
	CC		0.77	0.84	0.71
	Bias		2.46	0.27	0.89
WC	Mean	0.67	1.10	0.63	0.85
	CV	33.60	37.26	37.05	45.74
	CC		0.76	0.83	0.80
	Bias		0.43	-0.04	0.18

averaged rainy days (40–60 days), followed by the central and northern parts (20–50 days). The western parts received the least number of rainy days (less than 10 days). The region east of Lesotho, which lies on the windward side of the escarpment mountains (Fig. 1), experiences the maximum number of rainy days (50–70 days) in the country.

In general the model could reproduce the spatial distribution of the number of rainy days over the country, but with overestimated values. The overestimation of the number of rainy days is higher in KF scheme simulations (more than 70 days), followed by BMJ and GDE scheme simulations (60–70 days). However, rainy days generated by the BMJ scheme are spread over a larger area compared to GDE scheme. All convective parameterization schemes captured the area of the maximum number of rainy days east of Lesotho, but with various intensities. Interesting is that all schemes overestimated the number of rainy days to a higher degree over high orography, compared to lower lying areas, which indicates that the model has a bias in generating orography induced rainfall. The orography related rainfall bias is higher in KF scheme simulations compared to BMJ and GDE simulations. The performance by both the BMJ and GDE schemes seems to be superior, although the BMJ scheme has a slight advantage.

In order to investigate rainfall intensity of the daily rainfall that occurs over South Africa is divided into three rainfall categories (1) <10 mm day^{-1} (low rainfall) (2) 10–30 mm day^{-1} (moderate rainfall) and (3) >30 mm day^{-1} (high rainfall).

The spatial distribution of the DJF averaged (1991/1992–2010/2011) number of rainy days was analyzed according to these three categories (Fig. 15). It was found that areas with the maximum number of rainy days are predominantly associated with low intensities (low rainfall category). For example, the eastern parts of South Africa experienced 25–50 days in the low rainfall category, 6–12 days in the moderate rainfall category, and 1–2 days in the high rainfall category. The spatial distribution of the different intensities in rainfall is well captured by the model simulations, but mostly overestimated. This cer-tainly contributes to the overestimation of model simulated seasonal rainfall as illustrated in Fig. 3. However, some difference in rainfall category frequencies appears amongst the three cumulus parameterization schemes. Throughout the study it became evident that KF scheme simulations overestimated the amount and spatial distribution of rainfall compared to both observations and BMJ and GDE scheme simulations. However, KF scheme generated less rainy days in the low rain category compared to the GDE and BMJ schemes. The BMJ scheme yielded the highest number of rainy days in the low rainfall category with more than 55 days over a large part of the country, while the region of low rainfall for the KF and GDE schemes are more confined with values of 45–50 days. The KF scheme, however, generated patterns and rainy day values (more than 12 days and wide spread) similar to the BMJ and GDE schemes (about 12 days and more confined) in the moderate rainfall category. The BMJ scheme has better simulations in moderate rain rate category in terms of the spatial distribution, compared to the other two schemes. The intensity and spatial distribution of the number of rainy

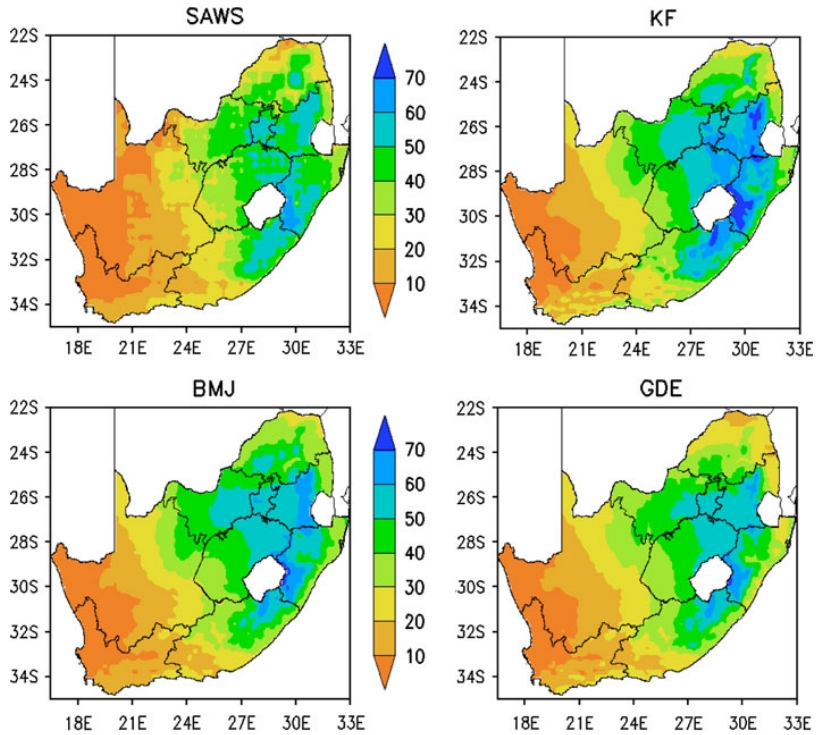

Fig. 14 Spatial patterns of the average number of rainy days from the same simulations as defined in Fig. 2. South Africa weather services (SAWS) observations were used for verification

days in the high rainfall category for the KF scheme are similar to its moderate rain values, although the number of rainy days is very high compared to the BMJ and GDE schemes, and mostly located over the east. The intensity and distribution of the number of rainy days in the high rainfall category are similar in both the BMJ and GDE schemes, with the highest values over the eastern coastal regions.

Despite of the fact that the model simulated rainy days with different rain rate categories is predominantly overestimated by all convective parameterization schemes, some interesting result appears when comparing the three simulations. The overestimation of seasonal rainfall over South Africa by the KF scheme (Fig. 3) (compared to the BMJ and GDE schemes) is mostly generated due to a higher number of rainy days in the moderate to high rainfall categories, especially over the eastern parts of the country, and in particular over the windward side of the eastern escarpment mountains. The smallest positive rainfall biases of the BMJ and GDE schemes could also be attributed to the higher number of rainy days in the moderate to high rainfall categories over the eastern parts of the country. Though there are differences in the number of rainy days between the BMJ and GDE schemes with different rainfall categories, both schemes generated similar mean seasonal rainfall (Fig. 2). This is due to compensation of rainfall between the low to moderate rainfall categories. More (less) rainy days from the low rainfall category compensates with less (more) rainy days from the moderate rainfall category in the BMJ scheme (GDE scheme) simulation. This indicates that the model simulations, although equal in climatology, might still not be uniform in terms of the number of rain days and rainfall categories generated.

7 Summary

In this study the performance of a high resolution (9 km) WRF model being driven by 0.75° ERA interim data over a period of 20 DJF seasons (1991/1992–2010/2011) is evaluated and its sensitivity to KF, BMJ and GDE convective schemes is studied. Comparing the model simulated rainfall with the SAWS observed rainfall, it is seen that the model could capture the east–west rainfall gradient over South Africa with all three schemes. However, the model simulated rainfall showed positive bias in simulating the rainfall with a maximum bias over the eastern high topographical region. Of the three cumulus schemes, KF simulated large positive biases over South Africa with BMJ simulating a more realistic climatology. The GDE scheme simulated dry bias over Limpopo region, though GDE

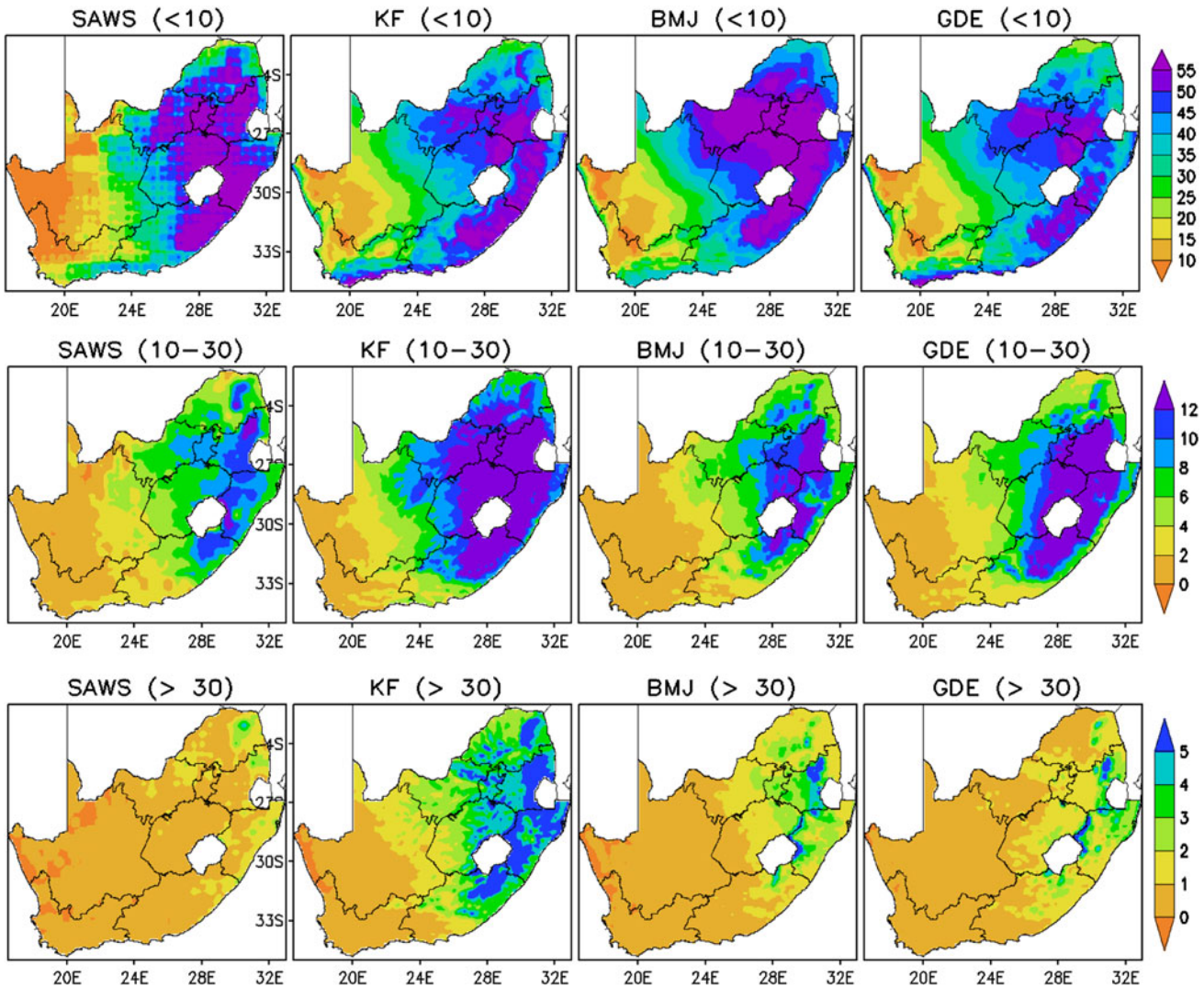

Fig. 15 Spatial patterns of the average number of rainy days from the same simulations as defined in Fig. 2, according to three rainfall intensity categories: (1) <10 mm day^{-1} = low rainfall (*top*), (2) 10–30 mm day^{-1} = moderate rainfall (middle) and (3) [30 mm day^{-1} = high rainfall (bottom). South Africa weather services (SAWS) observations were used for verification

simulated higher rainfall over parts of South Africa similar to BMJ scheme. The spatial correlation of rainfall between the model and simulations was the highest in both the KF and BMJ schemes, although statistical errors were higher in the KF scheme. Among the three schemes, the BMJ scheme appeared to generate rainfall that is closest to observations.

The biases in the spatial distribution of the rainfall were related to the biases in the vertically integrated moisture flux and its convergence. In the KF simulation, the moisture flux bias transports large moisture from the tropical region into South Africa causing a large area of moisture convergence and hence positive bias in rainfall over South Africa. In the BMJ simulation, the moisture flux bias from tropical region is such as to transport moisture out of the South Africa landmass. This leads to less moisture convergence compared to the KF simulation and hence less rainfall. The GDE simulated moisture flux is also in agreement with the rainfall distribution. The rainfall biases simulated by the different schemes are also in agreement with the stability of the atmosphere as simulated by the model.

The interannual variability in rainfall over southern Africa associated with ENSO was captured in the simulations accurately. This is an important outcome of the present study since some of the previous studies (Joubert et al. 1999; Engelbrecht et al. 2002; Hudson and Jones 2002; Boulard et al. 2012) had difficulties to reproduce the observed ENSO-southern Africa rainfall relationship in their regional climate modeling experiments. The present study has successfully reproduced the strength of observed ENSO–South Africa rainfall relationship over the period

1991/1992–2010/2011. The correlations among simulated rainfalls and Nino3.4 index were −0.66, −0.69 and −0.49 with KF, BMJ and GDE scheme respectively as compared to the observed correlation of −0.57. This study also successfully simulated most of the wet (dry) years that are associated with La Niña (El Niño). The improved simulation result in this study may be attributed to the high-resolution model configuration with 9 km resolution besides the role of better lateral boundary conditions taken from the reanalysis data. The model also showed good skill in simulating the excess rainfall over South Africa that is associated with positive subtropical IOD for the DJF season 2005/2006. A positive subtropical dipole helps moisture transports from Indian Ocean to southern Africa.

The excess and drought seasons simulated by KF scheme are stronger compared to the observations. The BMJ simulated the weaker wet season but the dry season is reasonably well simulated. GDE scheme simulated weak excess and drought season compared to the observations. In the case of drought season, widespread moisture divergence is seen in the observation. Moisture is transported away from the country towards the north. All the three schemes could simulate the similar pattern of moisture divergence and transport as observed. For the excess rainfall seasons, in observations, moisture convergence is usually seen over most part of the South Africa and moisture is mainly transported from the north. However, KF and BMJ show moisture transports, which are slightly weaker than the observations, from the north as well as southwest. GDE scheme doesn't show any moisture transport from the north but the only contribution is found from the southwest and simulated moisture convergence is weaker than the other two schemes. Among the nine provinces of South Africa, observed variability of rainfall is high over the NC but the variability is low over EC. LP receives a considerable amount of rainfall during the austral summer but has high interannual variability. It was noticed that the model has underestimated the magnitude of interannual variability for all the provinces except for WC province, where maximum rainfall occurs during the winter season.

A maximum number of rainy days are observed over the eastern region of the country followed by central and western regions. KF, BMJ and GDE could reproduce the spatial variability of number of rainy days accurately but overestimated the amplitude. The more number of rainy days compared to the observed rainy days in a season contributed to the positive bias of seasonal rainfall. The bias associated with KF is higher than the BMJ and GDE. Also, it was noted that the bias was higher in the high orography regions. This means that the model overestimated the orographic-related strong winds and instability of the atmosphere.

It is found that the stronger CAPE in KF and GDE has generated more convective rainfall and less stratiform rainfall. The weaker CAPE in BMJ produced less convective rainfall compared to the KF and GDE scheme. It was also interesting to note that the more convective unstable environment in KF and GDE produces more number of rainy days in moderate and high rain rate category. However, the less convective unstable environment in BMJ produces the maximum number of rainy days in low rain rate category compared to the KF and GDE. It was observed that the convective and stratiform rainfall simulated by BMJ scheme was close to the TRMM estimates. The KF and GDE scheme overestimated the convective rain and underestimated the stratiform rain.

A significant improvement in the simulation of the seasonal rainfall climatology and variability in climate models is crucial for making any further progress toward high-resolution seasonal predictions of summer rainfall over South Africa. This study has attempted to verify the fidelity of high resolution WRF model with three different cumulus parameterization schemes in terms of spatial distribution of rainfall and its variability over each province of the country. This is a hindcast study using the reanalysis data as a boundary condition, which will help us to know the merits/demerits over the model skill in reproducing the rainfall. However, real prediction from climate prediction models will be used as boundary conditions to produce the seasonal prediction of rainfall in a future study.

Acknowledgments This research is supported by the Japan Science and Technology Agency (JST)/Japan International Cooperation Agency (JICA) through Science and Technology Research Partnership for Sustainable Development (SATREPS). ERA interim data downloaded from ECMWF server is duly acknowledged. We appreciate the thoughtful comments from the anonymous reviewers.

References

Anthes RA, Kuo YH, Hsie EY, Low S, Bettge TW (1989) Estimation of skill and uncertainty in regional numerical models. Quart J Roy Meteor Soc 115:763–806

Barstad I, Sorteberg A, Flatøy F, Déqué M (2009) Precipitation, temperature and wind in Norway: dynamical downscaling of ERA40. Clim Dyn 33:769–776. doi:10.1007/s00382-008-0476-5

Behera SK, Yamagata T (2001) Subtropical SST dipole events in the southern Indian Ocean. Geophys Res Lett 28:327–330

Betts AK, Miller MJ (1986) A new convective adjustment scheme. Part II: single column tests using GATE wave, BOMEX, and arctic air-mass data sets. Quart J Roy Meteor Soc 112:693–709

Boulard D, Pohl B, Crétat J, Vigaud N (2012) Downscaling large-scale climate variability using a regional climate model: the case of ENSO over Southern Africa. Clim Dyn (published on line). doi:10.1007/s00382-012-1400-6

Caldwell PM, Chin H-NS, Bader DC, Bala G (2009) Evaluation of a WRF based dynamical downscaling simulation over California. Clim Change 95:499–521

Chen F, Dudhia J (2001) Coupling an advanced land-surface hydrology model with the Penn State-NCAR MM5 modeling system. Part I: model implementation and sensitivity. Mon Weather Rev 129:569–585
Cook KH (2000) The South Indian convergence zone and interannual rainfall variability over Southern Africa. J Clim 13:3789–3804
Cook KH (2001) A southern hemisphere wave response to ENSO with implications for southern Africa precipitation. J Atmos Sci 58:2146–2162
Crétat J, Pohl B (2012) How physical parameterizations can modulate internal variability in a regional climate model. J Atmos Sci 69:714–724
Crétat J, Richard Y, Pohl B, Rouault M, Reason CJC, Fauchereau N (2010) Recurrent daily rainfall patterns over South Africa and associated dynamics during the core of the austral summer. Int J Climatol 32:261–273
Crétat J, Macron C, Pohl B, Richard Y (2011) Quantifying internal variability in a regional climate model: a case study for Southern Africa. Clim Dyn 37:1335–1356
Crétat J, Pohl B, Richard Y, Drobinski P (2012) Uncertainties in simulating regional climate of Southern Africa: sensitivity to physical parameterizations using WRF. Clim Dyn 38:613–634
Dee DP et al (2011) The ERA-interim reanalysis: configuration and performance of the data assimilation system. Q J R Meteorol Soc 137:553–597
Dudhia J (1989) Numerical study of convection observed during the winter monsoon experiment using a mesoscale two-dimensional model. J Atmos Sci 46:3077–3107
Dyson LL (2009) Heavy daily-rainfall characteristics over the Gauteng Province. Water SA 35:627–638
Engelbrecht FA, Rautenbach CJdeW, McGregor JL, Katzfey JJ (2002) January and July climate simulations over the SADC region using the limited area model DARLAM. Water SA 28:361–373
Engelbrecht CJ, Engelbrecht FA, Dyson LL (2013) High-resolution model-projected changes in mid-tropospheric closed-lows and extreme rainfall events over southern Africa. Int J Climatol 33:173–187. doi:10.1002/joc.3240
Fauchereau N, Pohl B, Reason C, Rouault M, Richard Y (2009) Recurrent daily OLR patterns in the southern Africa/southwest Indian Ocean region, implications for South African rainfall and teleconnections. Clim Dyn 32:575–591
Giorgi F, Mearns LO (1999) Introduction to special section: regional climate modelling revisited. J Geophy Res 104:6335–6352
Gochis DJ, Shuttleworth WJ, Yang ZL (2002) Sensitivity of modeled North American monsoonal regional climate to convective parameterization. Mon Weather Rev 130:1282–1298
Grell GA, Dévényi D (2002) A generalized approach to parameterizing convection combining ensemble and data assimilation techniques. Geophys Res Lett 29:1693. doi:10.1029/2002GL015311
Heikkila U, Sandvik A, Sorterberg A (2011) Dynamical downscaling or ERA-40 in complex terrain using WRF regional Climate model. Clim Dyn 37:1551–1564. doi:10.1007/s00382-010-0928-6
Hong S-Y, Dudhia J, Chen S-H (2004) A revised approach to ice microphysical processes for the bulk parameterization of clouds and precipitation. Mon Weather Rev 132:103–120
Hudson DA, Jones RG (2002) Regional climate model simulations of present-day and future climates of southern Africa. Hadley centre technical note no 39, p 42
Janjic ZI (1994) The step-mountain eta coordinate model: further developments of the convection, viscous sublayer and turbulence closure schemes. Mon Weather Rev 122:927–945
Joubert AM, Katzfey JJ, McGregor JL, Ngunyen KC (1999) Simulating midsummer climate over southern Africa using a nested regional climate model. J Geophys Res 104:19015–19025
Jury MR (2012) An inter-comparison of model-simulated east–west climate gradients over South Africa. Water SA 38:467–478
Kain JS (2004) The Kain–Fritsch convective parameterization: an update. J Appl Meteorol 43:170–181
Kain JS, Fritsch JM (1993) Convective parameterization for mesoscale models: the Kain-Fritsch scheme. The representation of cumulus convection in numerical models. Meteorological monographs, vol 24. American Meteorological Society, pp 165–170
Kanamaru H, Kanamitsu M (2007) Fifty-seven-year California reanalysis downscaling at 10 km (CaRD10). part II: comparison with North American regional reanalysis. J Clim 20:5572–5592
Kanamitsu M, Kanamaru H (2007) Fifty-seven-year California reanalysis downscaling at 10 km (CaRD10) Part I. System detail and validation with observations. J Clim 20:5527–5552
Kgatuke MM, Landman WA, Beraki A, Mbedzi MP (2008) The internal variability of the RegCM3 over South Africa. Int J Clim 28:505–520
Landman WA, Kgatuke MM, Mbedzi M, Beraki A, Bartman A, du Piesanie A (2009) Performance comparison of some dynamical and empirical downscaling methods for South Africa from a seasonal climate modelling perspective. Int J Climatol 29:1535–1549. doi:10.1002/joc.1766
Leung LR, Mearns LO, Giorgi F, Wilby RL (2003) Regional climate research: needs and opportunities. Bull Am Meteorol Soc 84:89–95. doi:10.1175/BAMS-84-1-89
Lindesay JA (1988) South African rainfall, the southern oscillation and a southern hemisphere semi-annual cycle. J Climatol 8:17–30
Misra V (2003) The influence of Pacific SST variability on the precipitation over Southern Africa. J Clim 16:2408–2418
Mlawer E, Taubman S, Brown P, Iacono M, Clough S (1997) Radiative transfer for inhomogeneous atmosphere: RRTM, a validated correlated-k model for the long-wave. J Geophys Res 102:16663–16682
Mutemi JN, Ogallo LA, Krishnamurti TN, Mishra AK, Vijaya KTSV (2007) Multimodel based superensemble forecasts for short and medium range NWP over various regions of Africa. Meteorol Atmos Phys 95:87–113
Nicholson S, Kim J (1997) The relationship of El Niño–Southern Oscillation to African rainfall. Int J Climatol 17:117–135
Noh Y, Cheon WG, Hong SY, Raasch S (2003) The improvement of the K-profile model for the PBL using LES. Boundary Layer Meteorol 107:401–427
Ratna SB, Behera S, Ratnam JV, Takahashi K, Yamagata T (2013) An index for tropical temperate troughs over southern Africa. Clim Dyn 41:421–441. doi:10.1007/s00382-012-1540-8
Ratnam JV, Kumar KK (2005) Sensitivity of the simulated monsoons of 1987 and 1988 to convective parameterization schemes in MM5. J Clim 18:2724–2743
Ratnam JV, Behera S, Masumoto Y, Takahashi K, Yamagata T (2012) A simple regional coupled model experiment for summer-time climate simulation over southern Africa. Clim Dyn 39:2207–2217. doi:10.1007/s00382-011-1190-2
Ratnam JV, Behera SK, Ratna SB, Rautenbach H, Lennard C, Luo J–J, Masumoto Y, Takahashi K, Yamagata T (2013) Dynamical downscaling of austral summer climate forecasts over southern Africa using a simple regional coupled model. J Clim 26:6015–6032. doi:10.1175/JCLI-D-12-00645.1
Reason CJC, Jagadheesha D (2005) A model investigation of recent ENSO impacts over southern Africa. Meteor Atmos Phys 89:181–205
Reason CJC, Rouault M (2002) ENSO-like decadal variability and South African rainfall. Geophy Res Lett 29:1638. doi:10.1029/2002GL014663
Reason CJC, Allan RJ, Lindesay JA, Ansell TJ (2000) ENSO and climatic signals across the Indian Ocean basin in the global

context: part I, Interannual composite patterns. Int J Climatol 20:1285–1327
Richard Y, Trzaska S, Roucou P, Rouault M (2000) Modification of the Southern African rainfall variability/ENSO relationship since the late 1960s. Clim Dyn 16:883–895
Richard Y, Fauchereau N, Poccard I, Rouault M, Trzaska S (2001) XXth century droughts in southern Africa spatial and temporal variability, teleconnections with oceanic and atmospheric conditions. Int J Climatol 21:873–885
Rouault M, Richard Y (2005) Intensity and spatial extent of droughts in Southern Africa. Geophys Res Lett 32:L15702. doi:10.1029/2005GL022436
Skamarock WC, Klemp JB, Dudhia J, Gill DO, Barker DM, Duda M, Huang XY, Wang W, Powers JG (2008) A description of the advanced research WRF version 3. NCAR technical note, NCAR/TN\u2013475?STR, p 123
Soares PMM, Cardoso RM, de Medeiros J, Miranda PMA, Belo-Pereira M, Espirito-Santo F (2012) WRF high resolution dynamical downscaling of ERA-Interim for Portugal. Clim Dyn. doi:10.1007/s00382-012-1315-2
Tadross MA, Gutowski WJ, Hewitson BC, Jack C, New M (2006) MM5 simulations of interannual change and the diurnal cycle of southern African regional climate. Theor Appl Climatol 86:63–80
Uppala S, Dee D, Kobayashi S, Berrisford P, Simmons A (2008) Towards a climate data assimilation system: status update of ERA interim. ECMWF Newsl 115:12–18
van Heerden J, Taljaard JJ (1998) Africa and surrounding waters. Meteorology of the southern hemisphere, meteorological monographs, no. 49. American Meteorological Society, pp 141–174
Vigaud N, Pohl B, Crétat J (2012) Tropical-temperate interactions over Southern Africa simulated by a regional climate model. Clim Dyn (published on line). doi:10.1007/s00382-012-1314-3
Washington R, Preston A (2006) Extreme wet years over southern Africa: role of Indian Ocean sea surface temperatures. J Geophys Res 111:D15104. doi:10.1029/2005JD006724